Delft University of Technology

Document Version
Final published version

Licence
CC BY

Citation (APA)
Bakels, L., Wang-Erlandsson, L., van der Ent, R., Staal, A., Keys, P. W., Zemp, D. C., Fetzer, I., Taniguchi, M., & Gordon, L. J. (2026). Enhanced Dry Season Moisture Recycling in the Congo and Amazon Rainforests. *Water Resources Research*, *62*(9), Article e2025WR043039. https://doi.org/10.1029/2025WR043039

Important note
To cite this publication, please use the final published version (if applicable).
Please check the document version above.

Copyright
In case the licence states “Dutch Copyright Act (Article 25fa)”, this publication was made available Green Open Access via the TU Delft Institutional Repository pursuant to Dutch Copyright Act (Article 25fa, the Taverne amendment). This provision does not affect copyright ownership.
Unless copyright is transferred by contract or statute, it remains with the copyright holder.

Sharing and reuse
Other than for strictly personal use, it is not permitted to download, forward or distribute the text or part of it, without the consent of the author(s) and/or copyright holder(s), unless the work is under an open content license such as Creative Commons.

Takedown policy
Please contact us and provide details if you believe this document breaches copyrights.
We will remove access to the work immediately and investigate your claim.

This work is downloaded from Delft University of Technology.

Check for updates

Water Resources Research

RESEARCH ARTICLE
10.1029/2025WR043039

Enhanced Dry Season Moisture Recycling in the Congo and Amazon Rainforests

Lucie Bakels[1,2], Lan Wang-Erlandsson[1,2,3,4], Ruud van der Ent[5], Arie Staal[6], Patrick W. Keys[7], Delphine Clara Zemp[8], Ingo Fetzer[1,2], Makoto Taniguchi[3], and Line J. Gordon[1]

[1]Stockholm Resilience Centre (SRC), Stockholm University, Stockholm, Sweden, [2]Bolin Centre for Climate Research, Stockholm University, Stockholm, Sweden, [3]Research Institute for Humanity and Nature (RIHN), Kyoto, Japan, [4]Potsdam Institute for Climate Impact Research (PIK), Member of the Leibniz Association, Berlin, Germany, [5]Department of Water Management, Delft University of Technology, Delft, The Netherlands, [6]Copernicus Institute of Sustainable Development, Utrecht University, Utrecht, The Netherlands, [7]Department of Earth & Environment, Boston University, Boston, MA, USA, [8]Faculty of Sciences, Institute of Biology, University of Neuchatel, Neuchatel, Switzerland

Abstract The rainforests of South America and Africa are considerably reliant on rainfall supplied by evaporation from the rainforests themselves through moisture recycling. Thus, rainforest loss in these areas can reduce evaporation as well as subsequent rainfall in the wider forested region. During dry periods, a dampened water cycle may potentially aggravate rainforest water stress. However, few studies have investigated dry-period moisture recycling statistics within rainforests over longer records and consistently compared the rainforest moisture recycling in both continents. Here, we analyze dry-season anomalies of moisture recycling for mean-years and dry-years, in the South-American (Amazon) and African (Congo) rainforests over the years 1980–2023. We find that dry-season rainfall reliance on rainforest moisture increases slightly, but statistically significantly, by 5% (from a mean annual of 21% to 22%) in the Amazon and up to 12% (from 24% to 27%) in the Congo. At the same time, a lower fraction of rainforest evaporation stays within the rainforest during the dry season: 21% less from the Amazon (from 41% to 32%) and 22% less from the Congo rainforest (from 32% to 25%), which further decreases with increasing dryness. In response, areas downwind of the rainforests gain a higher dependency on rainforest moisture during dry seasons, amplified during dry years. For example, rainforest-sourced rainfall in Ecuador increases from ~25% annually to ~33% in the dry season. The findings highlight the critical role of rainforests in maintaining rainfall during periods when water is already scarce.

Plain Language Summary A substantial share of the rainfall in the tropical rainforests of South America (Amazon) and Africa (Congo) originates from moisture evaporated from the rainforests themselves. This means that rainforest loss can reduce evaporation, weaken the water cycle, and increase the risk of drought—both locally and in downwind areas. Few studies have analyzed and compared how the two rainforests contribute moisture to their own rainfall during dry periods. In this study, we analyze over four decades of data (1980–2023) to assess dry-season moisture recycling in both rainforests. We find that during dry seasons, rainforests become more reliant on their own moisture: self-generated rainfall increases by about 5% in the Amazon and 12% in the Congo. At the same time, a smaller share of rainforest evaporation returns as rainfall within the rainforest, especially in drier years. As a result, nearby regions become more dependent on rainforest moisture during dry seasons. For example, rainforest-sourced rainfall in Ecuador increases from ~25% annually to ~33% in the dry season. These findings highlight the critical role of intact rainforests in maintaining rainfall during periods when water is already scarce.

Lucie Bakels and Lan Wang-Erlandsson contributed equally to this work.

Key Points:

- Amazon and Congo rainforests recycle 21%–24% of their rainfall and retain 32%–41% of their evaporation locally
- During the boreal summer dry season, rainforest moisture self-reliance increases by a relative 5% in the Amazon and 12% in the Congo
- Rainforest moisture dependence is high in several countries, up to 32% annually and 36% during dry season in Peru

Supporting Information:

Supporting Information may be found in the online version of this article.

Correspondence to:

L. Wang-Erlandsson,
lan.wang@su.se

Citation:

Bakels, L., Wang-Erlandsson, L., van der Ent, R., Staal, A., Keys, P. W., Zemp, D. C., et al. (2026). Enhanced dry season moisture recycling in the Congo and Amazon rainforests. *Water Resources Research*, *62*, e2025WR043039. https://doi.org/10.1029/2025WR043039

Received 4 DEC 2025
Accepted 5 AUG 2026

Author Contributions:

Conceptualization: Lucie Bakels, Lan Wang-Erlandsson, Ruud van der Ent, Arie Staal, Patrick W. Keys, Delphine Clara Zemp, Line J. Gordon
Formal analysis: Lucie Bakels, Lan Wang-Erlandsson
Funding acquisition: Lan Wang-Erlandsson, Makoto Taniguchi, Line J. Gordon
Investigation: Lucie Bakels, Lan Wang-Erlandsson

© 2026 The Author(s). *Water Resources Research* published by Wiley Periodicals LLC on behalf of American Geophysical Union.
This is an open access article under the terms of the Creative Commons Attribution License, which permits use, distribution and reproduction in any medium, provided the original work is properly cited.

1. Introduction

The tropical rainforests of the Amazon and Congo are hotspots of global biodiversity (Pimm et al., 2014) and critical for the global carbon cycle (Hubau et al., 2020; Mitchard, 2018), as well as moisture suppliers of rainfall through a high root-uptake of soil moisture, transpiration used in photosynthesis, and interception of rainfall on surfaces such as canopies, stems, epiphytes, and litter (Crockford & Richardson, 2000; Gash, 1979; Gerrits et al., 2010; Pypker et al., 2006). The process of evaporation (both from transpiration, interception, and soil moisture evaporation) returning as rainfall is termed moisture recycling, and is a critical feedback for sustaining the regional hydroclimate of the rainforests. The importance of moisture recycling in the rainforests has been

19447973, 2026, 9, Downloaded from https://agupubs.onlinelibrary.wiley.com/doi/10.1029/2025WR043039 by Technical University Delft, Wiley Online Library on [10/09/2026]. See the Terms and Conditions (https://onlinelibrary.wiley.com/terms-and-conditions) on Wiley Online Library for rules of use; OA articles are governed by the applicable Creative Commons License

Methodology: Lucie Bakels, Lan Wang-Erlandsson, Ruud van der Ent, Arie Staal, Patrick W. Keys, Delphine Clara Zemp, Ingo Fetzer
Project administration: Lan Wang-Erlandsson
Supervision: Lan Wang-Erlandsson
Validation: Lucie Bakels
Visualization: Lucie Bakels, Lan Wang-Erlandsson
Writing – original draft: Lucie Bakels, Lan Wang-Erlandsson
Writing – review & editing: Lucie Bakels, Lan Wang-Erlandsson, Ruud van der Ent, Arie Staal, Patrick W. Keys, Delphine Clara Zemp, Ingo Fetzer, Makoto Taniguchi, Line J. Gordon

known for many decades (Salati et al., 1979). Current estimates of the percentage of forest rainfall with forest origin range around 24%–45% for the Amazon (Burde et al., 2006; Zemp et al., 2014, respectively), and around 28%–70%% in Congo (Dyer et al., 2017; Worden et al., 2024, respectively). In some parts of the Amazon and Congo rainforests, the percentage of precipitation from land can be up to 60%–80%, that is, the majority of the mean annual rainfall originates from terrestrial evaporation (Dominguez et al., 2022; Dyer et al., 2017; Spracklen et al., 2012; van der Ent et al., 2010).

The high moisture recycling rates can be both a boon and a bane for forest resilience: retained vegetation transpiration helps buffer against droughts by providing moisture for subsequent rainfall (Staal et al., 2018), while long-term moisture flow disruptions can lead to self-amplified forest loss (Wunderling et al., 2022; Zemp et al., 2017). Dry periods are the most critical, given that studies suggest that the dry season length in both the Amazon and Congo forests is increasing (Fu et al., 2013; Jiang et al., 2019) while at the same time, the rainforests are becoming increasingly vulnerable to repeated droughts (Tao et al., 2022).

In the Amazon, stronger regional forest-rainfall relationships during dry periods have been suggested to increase the negative effects of deforestation for forest resilience (Bagley et al., 2014; Staal et al., 2018) and agriculture production (Leite-Filho et al., 2021). Furthermore, due to a nonlinear relationship between atmospheric moisture content and rainfall, a minor decrease in moisture content could drastically reduce rainfall (Baudena et al., 2021). However, studies have contrasting conclusions for temporal variations of the extent to which rainforests depend on their own moisture supply for rainfall, which may be explained by differences in the selection of study regions, the methods, assumptions, and the time period considered (overview in Tables S2 and S3 of Supporting Information S1).

In the Amazon, some atmospheric moisture studies suggest that moisture recycling within the rainforest (rainforest moisture self-reliance) is highest in the dry season (Angelini et al., 2011; Claros et al., 2025; Dominguez et al., 2022; Eltahir & Bras, 1994; Staal et al., 2018; Yang & Dominguez, 2019; Zemp et al., 2014), while others suggest the wet season (Burde et al., 2006; Satyamurty et al., 2013). Consistent with a higher moisture self-reliance during the dry season, using a combination of satellite data, reanalysis data, and Lagrangian transport modeling, Spracklen et al. (2012) showed that deforestation leads to a greater reduction in rainfall in the dry season (−21% change) than in the wet season (−12% change). Dry season moisture self-reliance (in percent) has been shown to be about 7% higher during the two mega-drought years 2005 and 2010 relative to wet years (Bagley et al., 2014). Such dry-year dry-season anomalies are important to understand, as any marginal increase in water deficit during the dry season can have a large impact, for example, on streamflow and carbon balance (Mitchard, 2018; Marengo et al., 2011).

Estimates of moisture recycling within the Congo rainforest also vary. Pokam et al. (2012) reported the highest ratios during both dry seasons December–February and June–August for a rectangular region mainly in the forested regions. Dyer et al. (2017), who selected a rectangular box over the region, observed the highest ratio during the June–August dry season, but below-average ratios during the other dry season December–February. In contrast, Sorí et al. (2017), who used the basin delineation, suggest that within the basin, moisture self-reliance is highest in the rainy season, and below average in the dry season month of July. While discrepancies remain regarding the spatio-temporal variability of continental moisture recycling in the Congo, higher rainfall dependency on terrestrial evaporation sources in dry seasons is also indicated by isotope studies (Worden et al., 2021).

Moisture that reaches the forests is shaped by the full trajectory of air masses and the land types they traverse (e.g., Spracklen et al., 2012), and therefore depends both on shifts in the atmospheric circulation and on physiological traits of upwind areas. Increased forest moisture recycling rates during dry periods have been associated with reduced oceanic moisture inflow, and increased forest transpiration due to higher incoming radiation and forests' higher buffering capabilities through the ability to store and access subsoil water (Bagley et al., 2014; Costa et al., 2010; O'Connor et al., 2021; Staal et al., 2018; Zemp et al., 2014). However, this buffering capacity is increasingly threatened by deforestation and intensifying droughts, as shown, for example, in Rondônia (Mu et al., 2023). In the Amazon, high evaporation has also been associated with the presence of low-level jets during the dry season (do Nascimento et al., 2016), while in the Congo basin, weakened forest moisture recycling ratios in dry years have been attributed to a vertically integrated moisture flux divergence that favors moisture export from the basin (Sorí et al., 2017). However, questions remain with regard to the respective attribution of moisture recycling anomalies to either anomalies in wind patterns or evaporation, including a quantification of buffering

19447973, 2026, 9, Downloaded from https://agupubs.onlinelibrary.wiley.com/doi/10.1029/2025WR043039 by Technical University Delft, Wiley Online Library on [10/09/2026]. See the Terms and Conditions (https://onlinelibrary.wiley.com/terms-and-conditions) on Wiley Online Library for rules of use; OA articles are governed by the applicable Creative Commons License

capabilities of upwind land-use types, which, for example, can be relevant for understanding deforestation impacts on forest rainfall.

Comparing the Amazon and Congo rainforests offers valuable insights into how tropical rainforests function as moisture recycling systems under different climatic and geographic conditions. While both forests are major suppliers of moisture, they differ in their spatial heterogeneity and atmospheric circulation dynamics. The Amazon forest is mainly located in lowlands (between 0 and 400 m above sea level), bounded by the Andes in the west, and has a humid equatorial climate with minimal seasonal temperature variation (see Costa et al., 2021; Eamus et al., 2016, and references therein). The Inter-Tropical Convergence Zone (ITCZ) lies south of or over the Amazon forest from December to February, and then shifts northward, driving a pronounced dry season over the Amazon between June and September whose duration and strength vary across the region (Garreaud et al., 2009; Horel et al., 1989). The Congo rainforest is located at altitudes ranging from below 300 m in the center and higher. It has two dry seasons, and its climate is more variable and may be shaped by a combination of seasonally shifting circulation and associated moisture convergence, together with a strong land-atmosphere coupling over the forest (Longandjo & Rouault, 2024). Because moisture recycling in the Amazon and Congo is often examined in different studies with different methodologies, cross-comparisons between the two major rainforest systems often cannot be easily made. Despite the importance of rainfall for rainforest functioning and resilience (e.g., Singh et al., 2022), we still have limited knowledge of how variations in moisture recycling within the rainforest (i.e., rainforest moisture self-reliance) may potentially interact with dry periods and deforestation to impact forest rainfall, and how this process might differ between the Amazon and Congo.

This study aims to estimate dry period anomalies of rainforest moisture recycling in South America and Africa, and investigate the role of atmospheric circulation and land-use for the anomalies. Based on Eulerian atmospheric moisture tracking of rainforest moisture sources and sinks over 40 years in combination with Lagrangian transport modeling, we address the following specific questions: (a). What are the dry period anomalies of rainforest moisture sources and sinks, and do dry period anomalies increase with increasing dryness? (Section 3); (b). How are dry season anomalies linked to changes in circulation patterns (Section 4); (c). How do different land-use types buffer reduced moisture flows into the rainforest? (Section 5), and iii. How much do countries and their forested areas rely on recycled moisture from rainforests during dry periods compared to the annual average (Section 6). The dry periods investigated are the average dry seasons and the dry seasons in dry years.

2. Materials and Methods

2.1. Data

For our investigations on moisture recycling, we used the following meteorological data from the ERA5 reanalysis at 0.5° × 0.5° resolution provided by the European Center for Medium Range weather Forecast (ECMWF) (Hersbach et al., 2020): specific humidity and zonal and meridional wind speed at 22 model levels from zero pressure to surface pressure at 1 hr resolution, and evaporation and precipitation data at 1 hr resolution of the period 1979–2024. Due to substantial differences between observational and reanalysis precipitation data over the Amazon (Polasky et al., 2025) and data uncertainties in the Congo rainforest (Nicholson & Klotter, 2021; Steinkopf & Engelbrecht, 2022), we also compared our results using precipitation from the Multi-Source Weighted-Ensemble Precipitation (MSWEP) v2 (Beck et al., 2019) at 3-hourly temporal resolution of the full available period (1979–2019). The data was originally in 0.25° × 0.25° spatial resolution, and upscaled to 0.5° × 0.5° using the xarray regrid package (Schilperoort et al., 2024).

To compute circulation anomalies, we used a Lagrangian reanalysis data set (LARA: Bakels, Blaschek, et al., 2025), which is a Lagrangian translation of the ERA5 reanalysis (Hersbach et al., 2020) created using the FLEXPART model (Bakels et al., 2024; Stohl et al., 1998).

We used the HILDA+ data set (Winkler et al., 2021) for determining land-use types. This data set contains 0.1° × 0.1° yearly surface data of 12 land-use types, of which 6 are forest types. We upscaled this data to give land-use type fractions on a 0.5° × 0.5° grid, consistent with our other data sets, keeping the fractions of each land-use type per gridcell intact.

For our selection of countries, we used the python module regionmask (Hauser et al., 2024) country mask at 1:110 scale as provided by Natural Earth (naturalearthdata.com, last access 17 October 2025).

19447973, 2026, 9, Downloaded from https://agupubs.onlinelibrary.wiley.com/doi/10.1029/2025WR043039 by Technical University Delft, Wiley Online Library on [10/09/2026]. See the Terms and Conditions (https://onlinelibrary.wiley.com/terms-and-conditions) on Wiley Online Library for rules of use; OA articles are governed by the applicable Creative Commons License

2.2. Moisture Recycling Model

The Eulerian moisture tracking model WAM2layers (Kalverla et al., 2025; van der Ent et al., 2014) was used to track moisture sources of precipitation and destination of evaporation for the Amazon and Congo rainforest. WAM2layers tracks atmospheric moisture from zero pressure to surface pressure in two layers at the interface between IFS levels 111 and 112. This boundary can therefore be at a much lower pressure over mountainous terrain than at sea-level. The model applies the water balance, and assumes the atmosphere is well mixed within each of the two atmospheric layers. To track where evaporation from a given region (source region) falls as precipitation (sink region), moisture is tracked forward as follows:

$$\frac{\partial S_{\text{tracked}}}{\partial t} = -\frac{\partial S_{\text{tracked}u}}{\partial x} - \frac{\partial S_{\text{tracked}}v}{\partial y} + E_{\text{tracked}} - P_{\text{tracked}} \pm F_{\text{vertical,tracked}} \quad (1)$$

where S_{tracked} is the tracked atmospheric storage in an atmospheric column in one layer, t is time, u and v are wind components in the x zonal and y meridional directions, E_{tracked} is tracked evaporation entering and P_{tracked} is precipitation leaving an atmospheric column in one layer, and $F_{\text{vertical,tracked}}$ is the tracked vertical moisture transport between the two atmospheric layers. Evaporation in this paper refers to the total of all types of upward going vapor flows (i.e., ocean evaporation, transpiration, interception evaporation, soil evaporation, and open water evaporation) (Miralles et al., 2020), and the terrestrial and rainforest evaporation flows that we track naturally preclude the ocean evaporation component. Backward tracking to determine the source of precipitation uses an analogous equation. We used WAM2layers to track moisture for the years January 1979 until October 2024, of which 1979 and 2024 were used as spin-up for the forward and backward tracking, respectively.

WAM2layers has been extensively used to characterize the fate and properties of the atmospheric branch of the water cycle (e.g., Benedict et al., 2021; Keys et al., 2014; Link et al., 2020; Xiao & Cui, 2021). The moisture tracking performance generally compares well with Lagrangian type multi-atmospheric-layers moisture tracking and regional climate model online tracking (Benedict et al., 2026; van der Ent et al., 2013), while being relatively computationally efficient. We used the latest version of the model as described in Kalverla et al. (2025).

2.3. Data Analyses

First, we selected the study regions based on rainforest cover, and defined the dry periods based on precipitation and climatological water deficit (Section 2.3.1). Second, we tracked and analyzed the spatial and temporal patterns of the rainforest moisture sources and sinks of the study regions using WAM2layers (Section 2.3.2). Third, we computed air-mass footprints in order to understand the role of circulation shifts in changes of moisture sources during dry season (Section 2.3.3).

2.3.1. Selection of Study Regions and Dry Periods

Moisture tracking was applied to 0.5° × 0.5° grid cells in South America and Africa with at least 85% tropical evergreen broadleaf forest cover (hereafter referred to as Amazon and Congo rainforests), both in 1979 and 2019, according to the HILDA+ data set (Winkler et al., 2021). Averaged over the entire study region, each of the two rainforests has a forest cover of more than 96%. Monthly variations of moisture recycling metrics are shown (in Section 3). We held the forest region static over time to avoid introducing bias from including different geographical regions across the study period.

The study regions were kept constant for the whole tracking period, but the time-varying land-use HILDA+ data set (see Section 2.1) was used to distinguish moisture-source land-use types in Section 5.

We consider (a) the anomaly of dry season in mean years compared to mean annual ("dry season anomaly"), and (b) the Pearson correlation coefficient between the anomaly and the drought index of that year (see below). We ensured the validity of using the Pearson correlation coefficient by checking for a linear relationship through visual inspection, verifying the absence of outliers beyond 3 standard deviations, and ensuring that Spearman coefficients do not deviate by more than 0.05. Based on the mean precipitation patterns in the study regions, we selected June to September as the dry season months for South America, and January-February and June–August for Africa, see Section 3 .

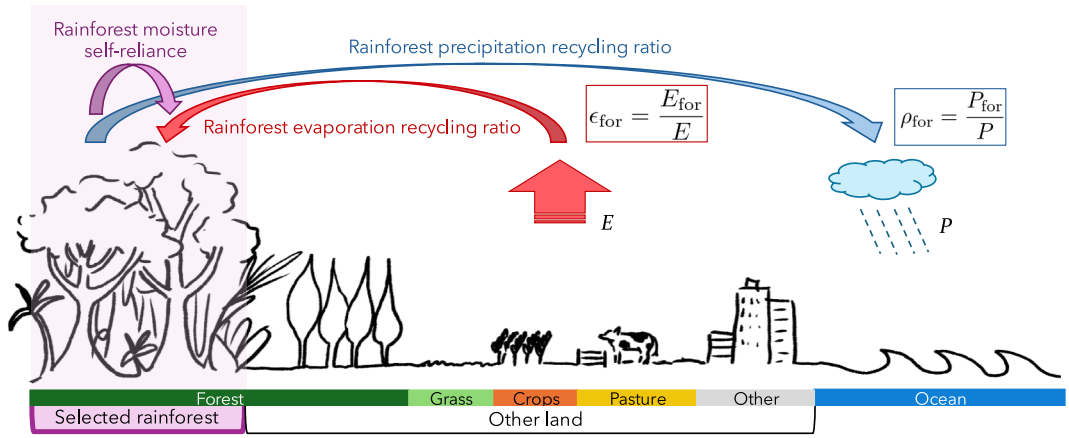


Figure 1. Conceptual figure showing moisture flows from and to the rainforest. Moisture evaporated from and precipitated back to the selected rainforest is referred to as rainforest moisture self-reliance. The fraction of evaporation from a certain area that ends up as precipitation over the selected rainforest is referred to as the "rainforest evaporation recycling ratio." The fraction of precipitation on a certain area that has a rainforest source, is referred to as the "rainforest precipitation recycling ratio".

We defined the dryness of a year by the intensity of maximum climatological water deficit (MCWD). The MCWD captures the drought years well: the list captures drought years for the Amazon that correspond to known drought years with potentially large effects on forests dynamics, 2005 and 2010 (e.g., Lewis et al., 2015), 2015 and 2016 (e.g., Yang et al., 2018), and 2023 (e.g., Marengo et al., 2024).

MCWD is defined as the most negative value of climatological water deficit Cm (mm), which is estimated based on monthly precipitation and a reference evaporation rate E_{ref} at 3.3 mm day^{-1} (used instead of actual E in order to represent the climatological drought) (Malhi et al., 2009; Zemp et al., 2017):

$$C_m = \min\left(0, C_{m-1} + \int_{d_{m,0}}^{d_{m,end}} P_{Y,m} - \int_{d_{m,0}}^{d_{m,end}} E_{ref}\right), \quad (2)$$

where m denotes the month number, $d_{m,0}$ and $d_{m,end}$ the first and last day of a month, $P_{Y,m}$ is the precipitation for year Y and month m, and C_0 is 0. The climatological water deficit C is accumulated continuously and reset to zero at the wettest month of the year, at which the next 12-month period calculation cycle starts (Malhi et al., 2009).

2.3.2. Moisture Recycling Analyses and Terminology

Figure 1 shows a conceptual overview of the different moisture flows we considered. The rainforest precipitation recycling ratio (i.e., the fraction of rainfall that originates from rainforest evaporation) is defined as:

$$\rho_{for} = \frac{P_{for}}{P}, \quad (3)$$

where P_{for} [L^{3}time^{-1} or L time^{-1}] refers to precipitation with rainforest origin. The ρ_{for} are estimated for all grid cells globally. The rainforest precipitation recycling ratio within the rainforest, that is, ρ_{for} values within the selected forested regions, will be referred to as the *rainforest moisture self-reliance*.

The terrestrial precipitation recycling ratio, denoted as ρ_{terr} [−], is defined as the fraction of rainforest precipitation that originate from evaporation from other land sources:

$$\rho_{terr} = \frac{\sum_{terr} E}{\sum_{sfor} P}, \quad (4)$$

19447973, 2026, 9, Downloaded from https://agupubs.onlinelibrary.wiley.com/doi/10.1029/2025WR043039 by Technical University Delft, Wiley Online Library on [10/09/2026]. See the Terms and Conditions (https://onlinelibrary.wiley.com/terms-and-conditions) on Wiley Online Library for rules of use; OA articles are governed by the applicable Creative Commons License

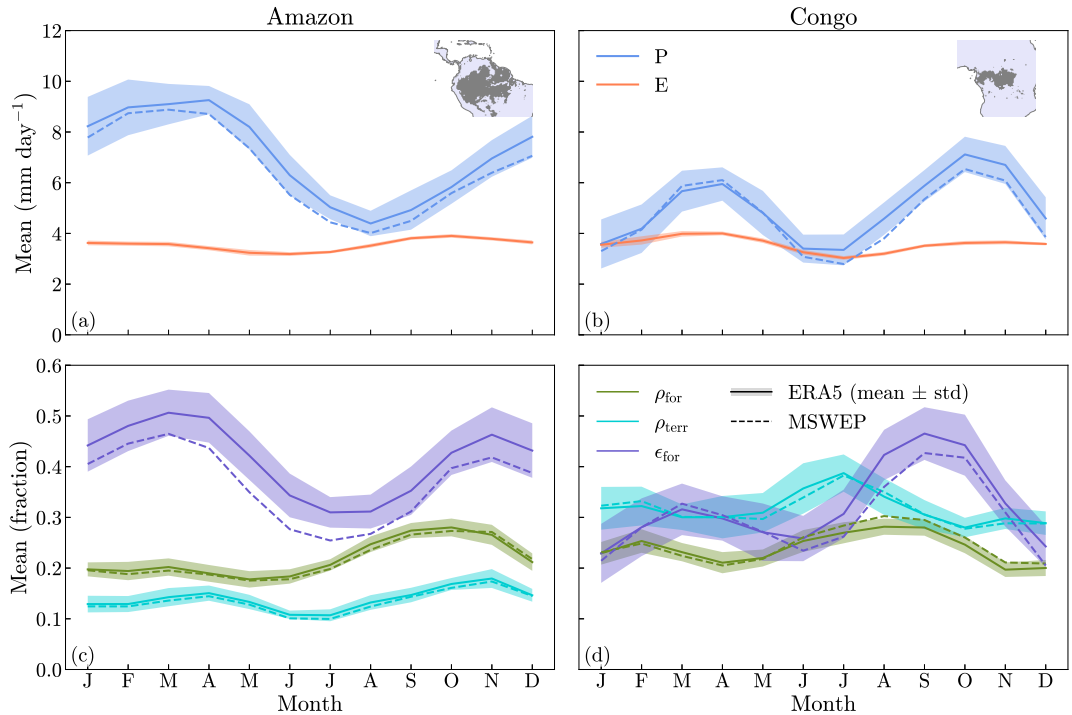


Figure 2. Monthly variations in precipitation for ERA5 (P, blue solid line) and MSWEP (P, orange solid line), and ERA5 evaporation (E, blue dashed line), fraction of precipitation from the rainforest (ρ_{for}, green/yellow solid line for ERA5/MSWEP), the fraction of precipitation that originates from land sources other than the selected rainforest (ρ_{terr}, green and yellow dotted lines), and fraction of evaporation to the rainforest (ϵ_{for}, green and yellow dashed lines) over the study period 1981–2017 for the total rainforest area (gray shaded areas in maps) in (a, c) the Amazon and (b, d) Congo. Shaded areas represent the standard deviation based on the annual variation. Note: considering the full 1980–2023 ERA5 period results in minimal differences.

where $\sum_{terr} E$ [L^{3}time^{-1} or L time^{-1}] denotes all evaporation from land outside of the selected rainforest at the global scale with a rainforest destination and $\sum_{sfor} P$ is the total rainforest precipitation.

Similarly, rainforest moisture dependence on oceanic sources, ρ_{ocean} [−], is defined as the fraction of rainforest precipitation that originate from evaporation from the ocean (E_{ocean} [L^{3}time^{-1} or L time^{-1}]):

$$\rho_{ocean} = \frac{\sum_{ocean} E}{\sum_{sfor} P}, \tag{5}$$

where $\sum_{ocean} E$ [L^{3}time^{-1} or L time^{-1}] is all oceanic evaporation with a rainforest destination and $\sum_{sfor} P$ is the total rainforest precipitation.

The rainforest evaporation recycling ratio (i.e., the fraction of evaporation that contributes to rainforest rainfall), ϵ_{for} [−], is defined as:

$$\epsilon_{for} = \frac{E_{for}}{E}, \tag{6}$$

where E_{for} [L^{3}time^{-1} or L time^{-1}] refers to evaporation that falls as rainfall in areas within the selected rainforest.

To see how these measures differ during the dry season, and if any (de-) amplification takes place during extra dry years, we both computed their absolute anomalies and computed the Pearson correlation coefficients between the annual values of these measures and the drought index of each year (MCWD).

19447973, 2026, 9, Downloaded from https://agupubs.onlinelibrary.wiley.com/doi/10.1029/2025WR043039 by Technical University Delft, Wiley Online Library on [10/09/2026]. See the Terms and Conditions (https://onlinelibrary.wiley.com/terms-and-conditions) on Wiley Online Library for rules of use; OA articles are governed by the applicable Creative Commons License

19447973, 2026, 9, Downloaded from https://agupubs.onlinelibrary.wiley.com/doi/10.1029/2025WR043039 by Technical University Delft, Wiley Online Library on [10/09/2026]. See the Terms and Conditions (https://onlinelibrary.wiley.com/terms-and-conditions) on Wiley Online Library for rules of use; OA articles are governed by the applicable Creative Commons License

2.3.3. Air-Mass Footprints

Anomalies in E_{for} can be caused by anomalies in E in the source region and/or by other meteorological conditions, such as regional wind patterns and rainfall generation in the sink region. To analyze the contribution of the circulation pattern anomalies to E_{for} anomalies, we compared the mean absolute volumetric E_{for} anomalies with air-mass transport anomalies.

To compute circulation anomalies, we used a Lagrangian reanalysis data set (LARA: Bakels, Blaschek, et al., 2025), which is a Lagrangian translation of the ERA5 reanalysis (Hersbach et al., 2020) created using the FLEXPART model (Bakels et al., 2024; Stohl et al., 1998). FLEXPART is a Lagrangian particle dispersion model (LPDM) that advances particles using ERA5 meteorological data and parameterizes subgrid convection and turbulence. For the creation of LARA, the entire atmosphere was discretized into particles of equal mass. These particles were initialized so that their number density was proportional to the air density. These air parcels were traced forward in time over 8-year periods between January 1980 and March 2024. Their positions and other properties are available at one-hour intervals.

For each month between 1980 and 2024, we selected all air parcels above the Amazon and Congo rainforests and traced them backwards over a period of 10 days, at an hourly temporal resolution. Each time an air parcel traveled below 1 km, its location was tagged as a potential moisture source. On average, this resulted in 10^9 and 6×10^8 separate instances per month for the Amazon and Congo, respectively.

We divided these instances by the 10-day integration period and by the total number of instances of air traveling below an altitude of 1 km to calculate the *fraction of rainforest-bound air mass*, or f_{air} hereafter. Using this metric, we calculated the fraction of air mass that originates from evaporation from the rainforest $\left(E_{for}/f_{air}\right)$.

Evaporation and circulation anomalies are expected to be important drivers of E_{for} anomalies, but they do not account for all the physical processes that are important for moisture transport (e.g., cloud formation, moisture rained out earlier/later). To indicate how much of the E_{for} anomalies are linked to changes in circulation, we calculated the following for the absolute dry-season evaporation anomalies with a rainforest destination $\left(\Delta E_{for}\right)$ and absolute air-mass footprint anomalies $\left(\Delta f_{air}\right)$:

- the Pearson correlation coefficient between: $r\left(\Delta f_{air}, \Delta E_{for}\right)$, where

$$\Delta X = X_{\text{dry-season}} - X_{\text{annual}}, \tag{7}$$

with $X \in \left\{f_{air}, E_{for}\right\}$;

- the fraction of gridcells that have a corresponding sign:

$$f_{\pm} = \frac{1}{N}\left|\left(\Delta f_{air,+} \cap \Delta E_{for,+}\right) \cup \left(\Delta f_{air,-} \cap \Delta E_{for,-}\right)\right|, \tag{8}$$

where N is the number of grid cells and ΔX_+ and ΔX_- positive and negative anomalies, respectively.

Additionally, to measure the possible amplification or reduction of the impact of circulation changes with increasing dryness, we calculated the Pearson correlation coefficient between MCWD and the annual correlation between the dry season anomaly and the air-mass footprint anomaly: $r\left[\text{MCWD}, r\left(\Delta f_{air}, \Delta E_{for}\right)\right]$.

3. Moisture Recycling Characteristics

The mean annual fraction of rainforest precipitation that originates from rainforest moisture sources (ρ_{for}) is similar between the Amazon (0.213 ± 0.007) and the Congo (0.237 ± 0.007) (Table 1, Table 2), although it follows different patterns throughout the seasons (Figure 2). The terrestrial precipitation recycling ratio ρ_{terr}, that is, the fraction of precipitation that originate from evaporation from non-selected-rainforest land sources, is considerably higher in the Congo (0.31 ± 0.01) than in the Amazon (0.140 ± 0.005). This difference reflects the influence of the prevailing westerly winds, which transport more air masses over land before reaching the Congo (Figure 4a), in contrast to the Amazon, which lies adjacent to the eastern coast of South America and receives

19447973, 2026, 9, Downloaded from https://agupubs.onlinelibrary.wiley.com/doi/10.1029/2025WR043039 by Technical University Delft, Wiley Online Library on [10/09/2026]. See the Terms and Conditions (https://onlinelibrary.wiley.com/terms-and-conditions) on Wiley Online Library for rules of use; OA articles are governed by the applicable Creative Commons License

Table 1
Moisture Recycling Measures of the Amazon Rainforest Divided by Their Moisture Source: Selected Rainforest, Other Land, and Ocean

Variable ERA5 1980–2023 (MSWEP 1981–2017)	Mean full period	Dry season anomaly full period	Annual r(mean, Y_{MCWD})	Annual r(dry mean, Y_{MCWD})
Selected rainforest				
ρ_{for}	0.213 ± 0.007 (0.210 ± 0.007)	**0.01** (**0.01**)	0.24 (0.29)	0.03 (0.19)
ϵ_{for}	0.41 ± 0.02 (0.37 ± 0.02)	**−0.09** (**−0.09**)	**0.53** (**0.34**)	**0.73** (0.22)
$P_{for}/area_{for}$ (mm day^{-1} m^{-2})	1.50 ± 0.08 (1.38 ± 0.08)	**−0.37** (**−0.38**)	**0.55** (**0.40**)	**0.75** (**0.38**)
$E_{for}/area_{for}$ (mm day^{-1} m^{-2})	1.48 ± 0.08 (1.32 ± 0.07)	**−0.36** (**−0.35**)	**0.56** (**0.38**)	**0.75** (0.28)
E_{for}/f_{air} (mm day^{-1})	3.73 ± 0.15 (3.34 ± 0.14)	**−0.74** (**−0.76**)	**0.59** (0.20)	**0.71** (0.05)
Land other than the selected rainforest				
ρ_{terr}	0.140 ± 0.005 (0.134 ± 0.005)	**−0.02** (**−0.02**)	0.21 (−0.01)	**0.38** (0.05)
$E_{terr}/area_{for}$ (mm day^{-1} m^{-2})	0.97 ± 0.06 (0.87 ± 0.05)	**−0.36** (**−0.34**)	**0.45** (0.21)	**0.73** (0.28)
E_{terr}/f_{air} (mm day^{-1})	3.55 ± 0.17 (3.21 ± 0.12)	**−1.45** (**−1.38**)	**0.60** (−0.30)	**0.78** (0.19)
Ocean				
ρ_{ocean}	0.67 ± 0.01 (0.67 ± 0.01)	0.01 (**0.02**)	−0.21 (**−0.58**)	0.07 (−0.12)
$E_{ocean}/area_{for}$ (mm day^{-1} m^{-2})	4.53 ± 0.23 (4.22 ± 0.23)	**−1.30** (**−1.16**)	**0.32** (0.01)	**0.71** (0.25)
E_{ocean}/f_{air} (mm day^{-1})	8.30 ± 0.32 (7.73 ± 0.34)	**−1.92** (**−1.71**)	**0.33** (−0.01)	**0.71** (0.23)

Note. $Area_{for}$ is the area of the Amazon rainforest in m^2. An explanation of all other measures can be found in Section 2. The mean of the full period, Its dry season anomaly, as well as the correlation coefficients between the MCWD and the annual full-year and annual dry-season means are listed for each moisture recycling measure. Significant values are shown in bold and insignificant values are shown in gray. A value is considered significant if the dry season anomaly exceeds one standard deviation (based on the yearly values) and the p-value for r_{MCWD} is below 0.05. Green values indicate stronger dependence or higher values during the dry season or under drier conditions (i.e., negative correlations). Red values indicate weaker dependence or lower values during the dry season or under drier conditions (i.e., positive correlations).

more direct oceanic influence (Figure 3a). Similarly, evaporation sources are more concentrated in the east and sinks in the west of the rainforests, following predominant wind patterns. The absolute equivalents for Figures 3 and 4, showing E_{for} and P_{for}, can be found in the supplement (Figures S1 and S2 in Supporting Information S1).

Nevertheless, the main moisture source for both the Amazon and the Congo is the ocean, accounting for a fraction of 0.67 ± 0.01 (Table 1) and 0.49 ± 0.02 (Table 2), respectively. Note that these fractions do not exactly add up to 1, due to the differing definitions: ρ_{for} is based on precipitation traced forward, while both ρ_{terr} and ρ_{ocean} are based on evaporation sources traced backward. Notably, the fraction of rainforest evaporation that returns as rainforest rainfall (ϵ_{for}) is higher in the Amazon (0.41 ± 0.02) than in the Congo (0.32 ± 0.04). A difference is expected, given the larger extent of the Amazon rainforest ($\sim 5.2 \times 10^{12}$ km^2) compared to the Congo rainforest ($\sim 1.7 \times 10^{12}$ km^2), which provides more time and space for recycled moisture to precipitate within the region, and is further enhanced by the presence of the Andes, which can act as a barrier that keeps the moisture longer within the basin (e.g., Hoyos et al., 2018; Zemp et al., 2014). The smaller size of Congo rainforest suggests that it recycles more moisture internally per unit area than the Amazon forest, implying that deforestation of an equivalent land area could have a greater impact on the regional moisture recycling.

In dry seasons, as shown in the rainforest precipitation recycling ratio (ρ_{for}) and the terrestrial precipitation recycling ratio (ρ_{terr}) remain similar or slightly increase in both the Amazon and Congo (Tables 1 and 2). In contrast, the fraction of evaporation that becomes rainforest rainfall (ϵ_{for}) decreases significantly during the Amazon JJAS and Congo JF dry seasons. The ϵ_{for} during the Congo JJA season remains close to its annual mean. Spatially, anomalies in ϵ_{for} are fairly evenly distributed across the rainforests: significant negative anomalies of $\sim$0.09 and $\sim$0.07 cover most of the Amazon (JJAS; Figure 3c and ϵ_{for} in Table 1) and the Congo (JF; Figure 4c and ϵ_{for} in Table 2). During the Congo JJA dry season (Figure 4e), although small (±0.04), a dichotomy emerges between the north-western and south-eastern parts of the rainforest, summing up to a non-significant total anomaly.

19447973, 2026, 9, Downloaded from https://agupubs.onlinelibrary.wiley.com/doi/10.1029/2025WR043039 by Technical University Delft, Wiley Online Library on [10/09/2026]. See the Terms and Conditions (https://onlinelibrary.wiley.com/terms-and-conditions) on Wiley Online Library for rules of use; OA articles are governed by the applicable Creative Commons License

Table 2
Moisture Recycling Measures of the Congo Rainforest

Variable ERA5 1980–2023 (MSWEP 1981–2017)	Mean	JF anomaly	JJA anomaly	Annual r(mean, Y_{MCWD})	Annual r(JF, Y_{MCWD})	Annual r(JJA, Y_{MCWD})
Selected rainforest						
ρ_{for}	0.237 ± 0.007 (0.242 ± 0.008)	0.004 (−0.003)	**0.03** (**0.04**)	−0.02 (0.29)	−0.07 (0.20)	−0.19 (0.20)
ϵ_{for}	0.32 ± 0.04 (0.30 ± 0.03)	**−0.07** (**−0.05**)	0.01 (−0.02)	**0.81** (**0.74**)	**0.82** (**0.71**)	**0.81** (**0.44**)
$P_{for}/area_{for}$ (mm day^{-1} m^{-2})	1.16 ± 0.13 (1.12 ± 0.11)	**−0.26** (**−0.24**)	**−0.17** (**−0.21**)	**0.84** (**0.82**)	**0.85** (**0.79**)	**0.85** (**0.77**)
$E_{for}/area_{for}$ (mm day^{-1} m^{-2})	1.12 ± 0.13 (1.08 ± 0.10)	**−0.22** (**−0.17**)	−0.11 (**−0.17**)	**0.85** (**0.78**)	**0.85** (**0.76**)	**0.84** (**0.57**)
E_{for}/f_{air} (mm day^{-1})	3.52 ± 0.36 (3.37 ± 0.25)	**−0.36** (**−0.20**)	**−0.58** (**−0.77**)	**0.86** (**0.76**)	**0.77** (**0.69**)	**0.83** (**0.48**)
Land other than the selected rainforest						
ρ_{terr}	0.31 ± 0.01 (0.31 ± 0.01)	−0.01 (**0.01**)	**0.05** (**0.05**)	**0.32** (0.33)	−0.24 (−0.18)	−0.14 (−0.08)
$E_{terr}/area_{for}$ (mm day^{-1} m^{-2})	1.50 ± 0.19 (1.41 ± 0.15)	**−0.34** (**−0.23**)	−0.19 (**−0.28**)	**0.82** (**0.80**)	**0.86** (**0.74**)	**0.82** (**0.57**)
E_{terr}/f_{air} (mm day^{-1})	2.20 ± 0.26 (2.06 ± 0.20)	**−0.61** (**−0.46**)	−0.12 (**−0.28**)	**0.84** (**0.79**)	**0.68** (**0.52**)	**0.83** (**0.59**)
Ocean						
ρ_{ocean}	0.49 ± 0.02 (0.49 ± 0.02)	**0.07** (**0.09**)	**−0.02** (**−0.02**)	**−0.32** (−0.25)	−0.29 (−0.23)	−0.15 (−0.05)
$E_{ocean}/area_{for}$ (mm day^{-1} m^{-2})	2.22 ± 0.24 (2.10 ± 0.19)	**−0.28** (−0.10)	**−0.65** (**−0.74**)	**0.75** (**0.67**)	**0.82** (**0.67**)	**0.76** (**0.51**)
E_{ocean}/f_{air} (mm day^{-1})	6.57 ± 0.62 (6.21 ± 0.50)	−0.52 (0.03)	**−2.02** (**−2.25**)	**0.70** (**0.62**)	**0.53** (**0.39**)	**0.64** (**0.35**)

Note. The mean of the full period, their JF and JJA dry season anomalies, as well as the correlation coefficients between the MCWD and the annual full-year and both annual JF and JJA dry-season means are listed for each moisture recycling measure. Similar to Table 1, but now for the Congo rainforest.

Similarly, although absolute integrated values of ρ_{for} show little change across the rainforest, spatial anomalies (Figures 3d, 4d, and 4f) reveal marked differences in precipitation dependence patterns. In the Amazon, the northern and western borders, particularly near the Andes, show increased reliance on forest-sourced moisture, whereas the south-eastern parts become less reliant. This pattern is consistent with Hoyos et al. (2018), who found an enhanced redistribution of Amazonian moisture toward northwestern South America. In the Congo JJA season, spatial patterns of ρ_{for} anomalies are nearly the inverse of those during the JF season, reflecting seasonal wind reversals associated with shifts in the Inter-Tropical Convergence Zone (ITCZ). Rainforest moisture self-reliance is notably above average in the northern rainforest during JJA and below average during JF, by approximately 10 and 7 percentage points, respectively.

Correlations between rainforest dryness (MCWD) and both annual and dry-season ρ_{for} values show no significant amplification of rainforest moisture self-reliance during drier periods (Table 1, Table 2). However, all regions and seasons exhibit a strong correlation between MCWD and ϵ_{for}, indicating that a higher fraction of rainforest evaporation precipitates outside the rainforest under drier conditions.

In addition to the results derived using ERA5 precipitation data, Table 1, Table 2, and Figure 2 also show results based on MSWEP precipitation data at 3-hourly resolution between 1981 and 2017 (excluding spin-up years). Although not all values are statistically significant across both data sets, and some measures differ, the signs of anomalies and correlations generally agree and there are no significant contradictions. As shown in Figure 2, mean precipitation rates are lower in MSWEP for both the Amazon and Congo rainforests. Using the 1981–2017 period for both data sets yields lower mean precipitation rates of 0.5 mm day^{-1} for the Amazon and 0.3 mm day^{-1} for the Congo. ϵ_{for} is on average 0.05 and 0.02 lower in MSWEP than in ERA5 for the Amazon and Congo, respectively. Mean differences between MSWEP and ERA5 simulations for ρ_{for} and ρ_{terr} remain below one percentage point. Using the full 1980–2023 ERA5 period results in negligible changes in the mean values.

4. Air-Mass Footprint Anomalies

Rainfall over the rainforest depends on the inflow of moisture through the atmosphere, from evaporation from the ocean and other water bodies, or from land. In addition, the amount of moisture transported from each source depends on the atmospheric circulation, which is here represented by the air-mass footprint (see Section 2.3.3).

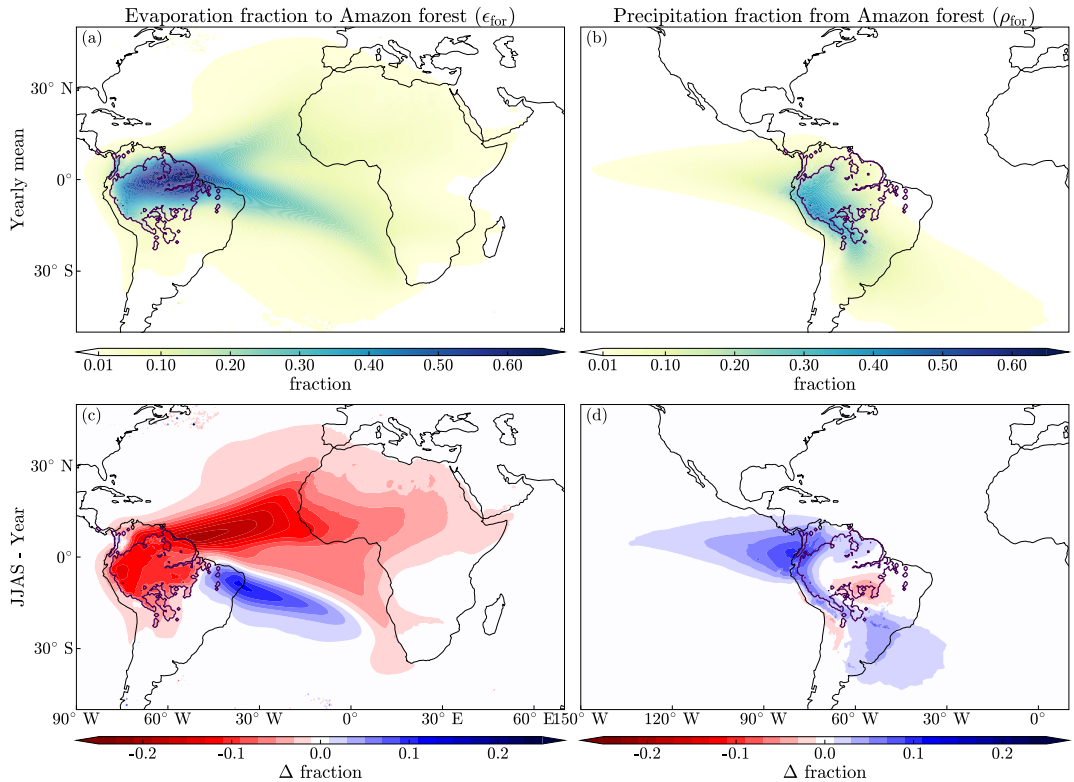


Figure 3. The fraction of evaporation destined for the Amazon rainforest (ϵ_{for}) and fraction of precipitation originating from the Amazon rainforest (ρ_{for}) at the (a, b) mean annual values, and their absolute anomalies in the (c, d) dry seasons (in fractional difference between the dry season and the mean annual). The purple lines denote the selected rainforest boundaries. For study region and time period selections, see Section 2.3.1, and for moisture recycling metrics definition, see Section 2.3.2.

The seasonal shift of the ITCZ significantly alters this air-mass footprint and, as previously suggested, is likely an important driver of the changes in moisture source regions during dry seasons (see Figures 3c and 4c–4f). This does not necessarily mean that rainfall variability is driven by the ITCZ, which was found to strongly depend on how moisture is locally converging in the atmosphere in the case of the Congo rainforest (Longandjo & Rouault, 2024).

Using the LARA data set, it becomes possible to quantify the link between the air mass footprint and the evaporation-to-precipitation source–sink relationship. We explore this by comparing anomalies in the air mass footprint and evaporation sources by computing the Pearson correlation coefficient between 2D maps of these values. A flowchart of our method can be found in the supplement (Figure S3 in Supporting Information S1) and mean anomalies of E_{for}, absolute E, and f_{air} are mapped in Figure S4 of Supporting Information S1. The Pearson coefficient uses the mean of each data set to compare them, losing information about the absolute comparison between the data sets, possibly skewing our results in favor of the importance of air-mass footprints. For this reason, we include the correspondence between signs of the two anomalies which can be found on the x-axes. High r-values together with high sign correspondence indicate that circulation anomalies play an important role for E_{for} anomalies.

For each dry season of the Amazon and Congo rainforest moisture sink regions, Figure 5 shows the correlations between dry-season air-mass footprint anomalies and dry-season moisture source anomalies, $r(\Delta f_{air}, \Delta E_{for})$, with respect to moisture sourced from the rainforest itself, from other terrestrial sources, and from the ocean. We find a strong positive correlation between dry-season air-mass-footprint anomalies over the ocean and E_{for} anomalies for all regions and dry seasons, and near-zero mean correlations between rainforest moisture source anomalies and circulation patterns. This is expected, as more local sources (within the rainforest) are more dependent on local processes and therefore less affected by the 10-day air-mass footprint, while distant sources (such as the ocean) are more sensitive to variations in long-range air-mass transport.

19447973, 2026, 9, Downloaded from https://agupubs.onlinelibrary.wiley.com/doi/10.1029/2025WR043039 by Technical University Delft, Wiley Online Library on [10/09/2026]. See the Terms and Conditions (https://onlinelibrary.wiley.com/terms-and-conditions) on Wiley Online Library for rules of use; OA articles are governed by the applicable Creative Commons License

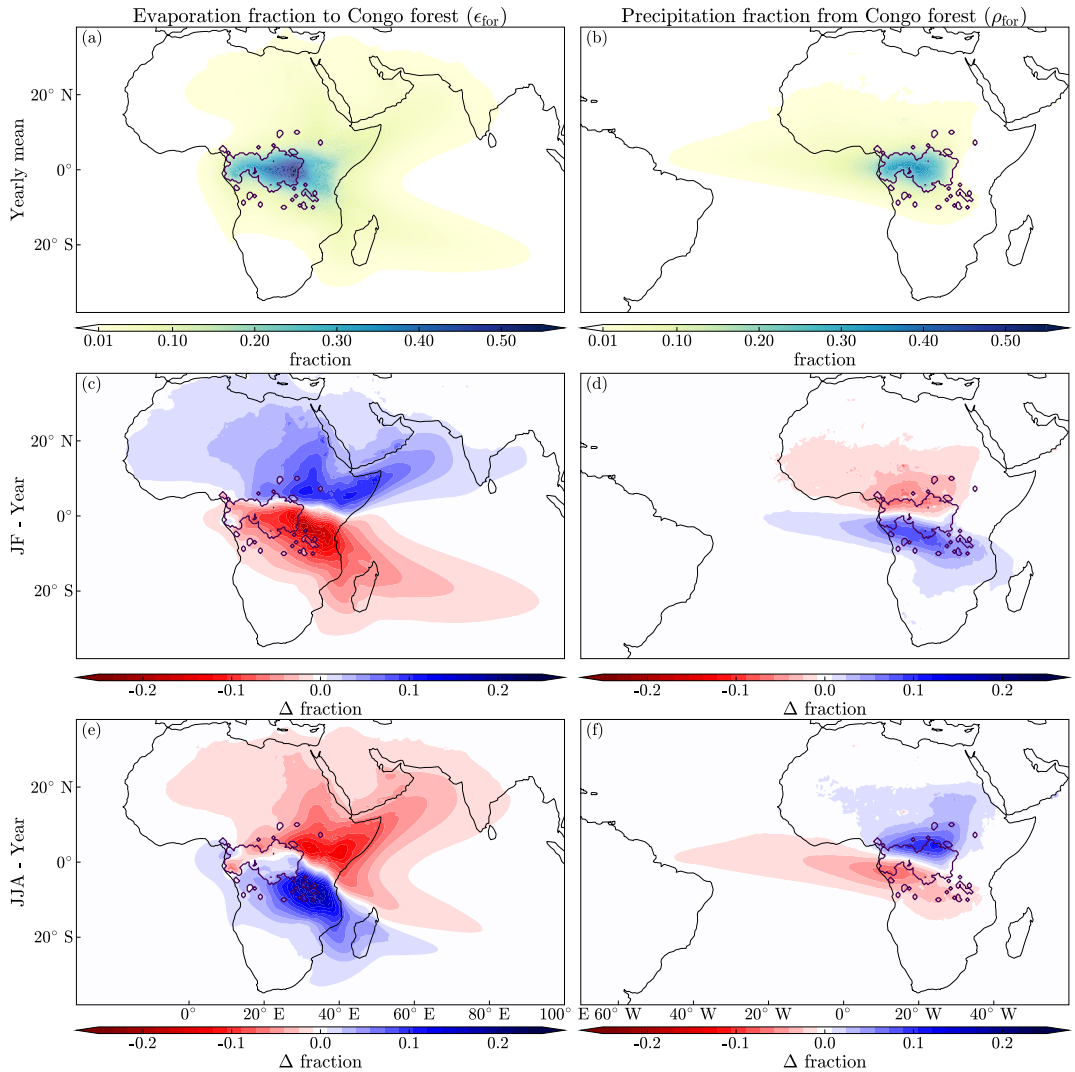


Figure 4. The fraction of evaporation that goes to the Congo rainforest and the fraction of precipitation originating from the Congo rainforest at the (a, b) mean annual scale, and their absolute anomalies in the (c, d) January-February (JF) dry season (i.e., difference between the JF and the annual mean), and (e, f) June–August (JJA) dry season (i.e., difference between the JJA and the mean annual). The purple lines denote the selected rainforest boundaries. For study region and time period selections, see Section 2.3.1, and for moisture recycling metrics definition, see Section 2.3.2.

In the Amazon (Figure 5a), all terrestrial sources (rainforest and other land) show near-zero mean correlation coefficients. However, the spread in yearly dry-season correlation values is large and correlates strongly with the dryness of the rainforest (MCWD). During wetter dry seasons, air-mass-footprint anomalies are more positively correlated with E_{for} anomalies, while during drier dry seasons, the two become even anti-correlated for rainforest sources. However, although these correlations are relatively strong and significant, the sign-correspondence, $f_{\pm}$, stays fairly constant at $\sim$0.5, independent of drought index, due to the dry-season anomalies over the whole selected rainforest area being negative. A similar, though less extreme, pattern is visible for land moisture sources other than the rainforest.

Interestingly, although strongly correlated overall, oceanic source anomalies become less correlated with circulation anomalies during drier dry seasons (i.e., years with higher MCWD values). For the Congo (Figures 5b and 5c), circulation anomalies are strongly correlated with moisture source anomalies over land, but not over the selected rainforest itself. However, their $f_{\pm}$ are low during JF (0.45). Correlations between the spread of $r(\Delta f_{air}, \Delta E_{for})$ and MCWD are less pronounced than in the Amazon. Increasing dryness does not appear to be clearly linked to changes in the role of circulation anomalies in driving moisture source anomalies. However, with

19447973, 2026, 9, Downloaded from https://agupubs.onlinelibrary.wiley.com/doi/10.1029/2025WR043039 by Technical University Delft, Wiley Online Library on [10/09/2026]. See the Terms and Conditions (https://onlinelibrary.wiley.com/terms-and-conditions) on Wiley Online Library for rules of use; OA articles are governed by the applicable Creative Commons License

10.1029/2025WR043039

19447973, 2026, 9, Downloaded from https://agupubs.onlinelibrary.wiley.com/doi/10.1029/2025WR043039 by Technical University Delft, Wiley Online Library on [10/09/2026]. See the Terms and Conditions (https://onlinelibrary.wiley.com/terms-and-conditions) on Wiley Online Library for rules of use; OA articles are governed by the applicable Creative Commons License

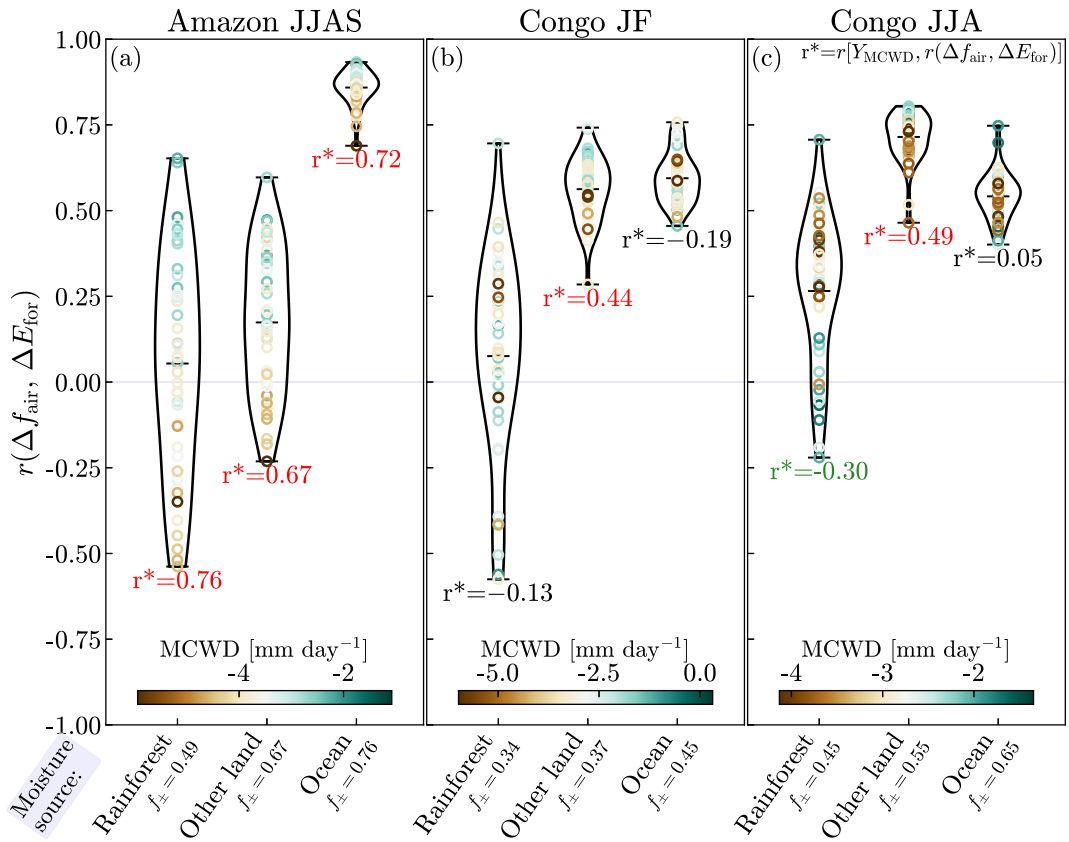


Figure 5. Correlation between dry season air-mass footprint anomalies (Δf_{air}) and dry season moisture source anomalies (ΔE_{for}) for each moisture source (rainforest, other land, ocean) and sink region: (a) Amazon JJAS, (b) Congo JF, and (c) Congo JJA (see Equation 7). The correlation of the anomalies of each year is separately plotted on top of the distribution and colored by its respective drought index MCWD. At the bottom of each individual violin plot, the correlation coefficient r^* between the MCWD and the correlation between the anomalies is given. Red values show a decreasing correlation between the anomalies with increasing drought, and increasing anomaly correlations with increasing dryness are shown in green. Insignificant correlations with p-values ≥0.05 are shown in gray. Mean sign-correspondence fractions between Δf_{air} and ΔE_{for} are shown on the x-axis as $f_{\pm}$ (see Equation 8) Results are shown for all years between 1980 and 2023 for the ERA5 simulations.

increasing dryness, the influence of circulation appears to weaken for terrestrial sources other than the selected rainforest, while becoming slightly stronger over the rainforest during the JJA season. This suggests that during increasingly dry JJA seasons, circulation anomalies over the rainforest align more closely with anomalies in evaporation that returns as precipitation within the rainforest.

Figure S5 in Supporting Information S1 shows the equivalent of Figure 5, but for correlations and sign correspondence within the different regions and source areas using absolute evaporation anomalies instead of air-mass transport anomalies. We find higher correlations and sign correspondence between absolute E and E_{for} within the Amazon forest source area. In the Congo rainforest, although the correlations are lower, we find a higher sign-correspondence across all source regions during JF. Values for all other regions and seasons are lower. The mean collinearity between air-mass transport anomalies and absolute evaporation anomalies are 0.2 and −0.2 for the Amazon and Congo, respectively. When we weight the absolute evaporation anomalies by the air-mass transport anomalies, we see how much of the forest-destined evaporation source anomalies can be explained by our method. This is shown in Figure S6 of Supporting Information S1. We find similar or higher correlations and sign-correspondence across all regions, but also that certain processes remain unexplained (e.g., cloud formation, moisture rained out earlier/later).

In the Amazon, the mean correlation values for the MSWEP simulations all terrestrial sources are somewhat lower: $r(\Delta f_{\text{air}}, \Delta E_{\text{for}}) = -0.02$ (Figure S7 in Supporting Information S1) instead of 0.05 for the rainforest in Figure 5a, and 0.05 instead of 0.09 for other land. For the Congo rainforest, mean values differ by less than 0.01,

except for other land sources during the JJA season, where MSWEP gives a mean correlation of 0.32 compared to 0.36 in ERA5 in Figure 5c. Correlations between MCWD and $r(\Delta f_{air}, \Delta E_{for})$ are generally lower for the MSWEP data (Figure S7 in Supporting Information S1). For the MSWEP results, Amazonian land sources other than the rainforest and oceanic sources are not statistically significant (p-value ≥ 0.05), as is also the case for other land sources during the Congo JJA season.

5. Land-Use Type

In addition to understanding the relationship between shifting circulation patterns and moisture transport, we also examine how seasonal and dryness-related fluctuations in moisture transport depend on the type of the moisture source. Specifically, we explore how different source-region types "buffer" the moisture flow toward the rainforests during dry seasons and with increasing rainforest dryness. We define the amount of "buffering" to be the fractional difference between the annual mean and dry-season mean moisture supply from each land-use type, that is, how stable the moisture flow is per land-use type. We use the time-varying land-use mask as described in Section 2. Due to shifting winds across seasons and substantial land-use changes over recent decades, we normalize the evaporation from each source by both the total area of the land-use type and the volume of air passing over that region with the potential to deliver moisture to the rainforests.

Figure 6 shows the moisture transported to the Amazon and Congo rainforests per air-mass unit, for each land-use type. Note that the "other forest" land-use type here only includes forest outside of the selected Amazon and Congo rainforest, and can be of any type. In the Amazon (Figure 6a), among all source-land-use types, other forest shows the smallest fractional decrease in absolute moisture contribution between the dry season and the annual mean (−0.37), whereas cropland (−0.55), pasture (−0.38), and grassland (−0.55) sources all show reduced buffering capacity. For the Congo rainforest (Figure 6b), which depends considerably more on non-oceanic moisture sources than the Amazon rainforest (see Figure 2), the picture is quite different. Dry-season means are much closer to annual means, and no clear difference in buffering emerges between land-use types.

Considering the air-mass footprints for different seasons (Figure 6b), which vary more strongly over land in the Congo than in the Amazon (Figure 6a), some results may be explained by shifts in where a given land-use type is located. For instance, during the JJA season, grassland shows a similar moisture-per-air-mass ratio (−0.04) to the annual mean, but the map reveals that less air is transported over the northern, drier grasslands. Instead, more air flows over the southern grasslands, which have expanded over time due to deforestation. The opposite is visible for the JF season, transporting more air over the northern grasslands. As a result, grassland buffers the moisture flow to the Congo rainforest well during the JJA dry season, but buffers the least during the JF dry season (−0.28), when more air is transported to the Congo rainforest from the north. A similar pattern appears for pastures (JJA: −0.03, JF: −0.27). Very similar fractional differences in E_{for}/f_{air} between dry-season and annual means are found when using the MSWEP simulations (Figure S8 in Supporting Information S1), with deviations for all land-use types within ±0.1.

In addition to fractional differences between dry-season and annual means, it is also important to assess how land-use types respond to increasing dryness, shown in Figures S9 and S10 in Supporting Information S1 (ERA5) (MSWEP). For the ERA5 simulation, all source-region types of the Amazon rainforest, with the exception of grassland, show similar correlations with the dryness index (MCWD), with significant Pearson correlation coefficients of ∼0.54−0.57 between MCWD and the fractional difference between dry-season and annual means (Figure S10 in Supporting Information S1). This would suggest that all land-use types, apart from grassland, show equal buffering-amplification for the selected Amazon rainforest. However, the MSWEP simulation results show no strong or significant correlations, making this result questionable (Figure S10 in Supporting Information S1). In the Congo, there are no strong or significant differences between dry-season and annual correlations with MCWD in either simulation.

6. Countries' Rainfall Reliance on Rainforest Moisture

As shown in Tables 1 and 2, during the dry season, a higher fraction of rainforest evaporation leaves the rainforest and precipitates elsewhere. This fraction increases with rainforest dryness (MCWD). In this section, we investigate where this moisture ends up, focusing on the dependence of different countries on rainforest-sourced rainfall. Figure 7 shows the precipitation dependence of a selection of countries on the rainforest, both

19447973, 2026, 9, Downloaded from https://agupubs.onlinelibrary.wiley.com/doi/10.1029/2025WR043039 by Technical University Delft, Wiley Online Library on [10/09/2026]. See the Terms and Conditions (https://onlinelibrary.wiley.com/terms-and-conditions) on Wiley Online Library for rules of use; OA articles are governed by the applicable Creative Commons License

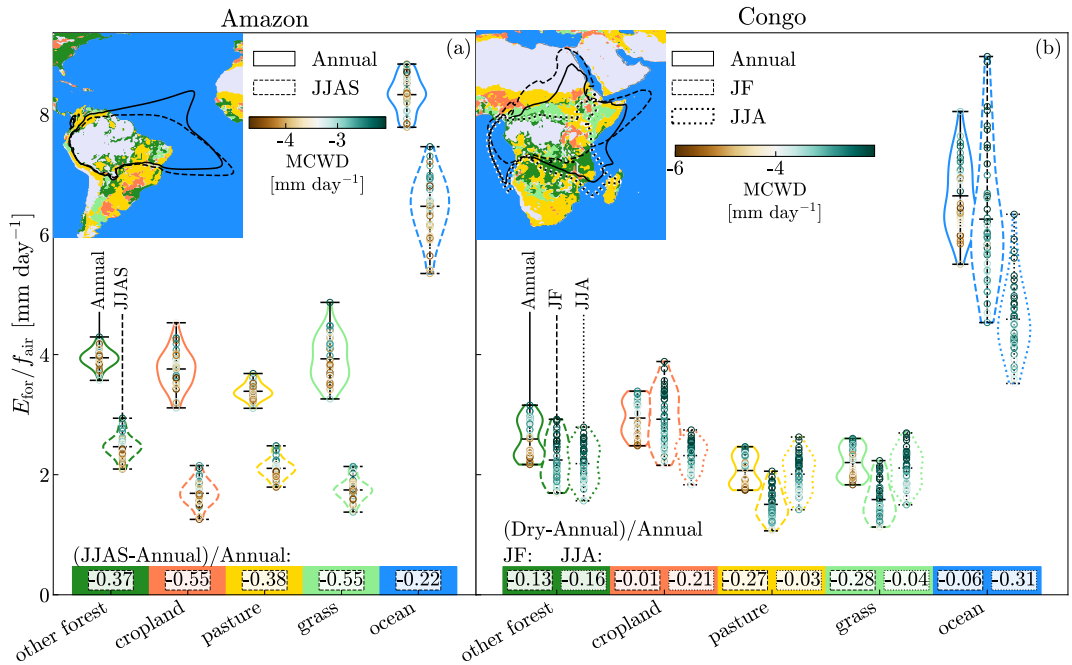


Figure 6. Moisture transported to the Amazon (a) and Congo (b) rainforests is shown per air-mass unit and moisture-source-region type. The moisture-source-region types considered are other forest (dark green), cropland (orange), pasture (yellow), grassland (light green), and ocean (blue). The spatial distribution of the source region types are shown on the maps in the upper left corner of each panel for the year 2000. The contour lines on the maps indicate the 75th percentile of the 10-day mass footprint for the period of 1980–2019. Results for each year are scattered individually on top of the violin plots and are colored according to the corresponding drought index (MCWD). Relative differences between dry season and annual means are listed for each source region type at the bottom of each panel. Note that forests here include all types of forest outside of the Amazon and Congo selected rainforest area. Results are shown for all years between 1980 and 2019 for the ERA5 simulations, later years are omitted due to the time-varying land mask (HILDA+) covering up to 2019.

annually and during the dry season, and whether this dependence is (de-) amplified with increasing rainforest dryness. Figure 8 shows a further breakdown of the fraction of this rainforest-sourced precipitation that falls on any forest type or other land-use types.

In South America (Figure 7a), the countries most dependent on Amazon-sourced moisture are located west of the rainforest. Peru shows the highest dependence on rainforest-sourced moisture, with ∼32% of its annual precipitation and ∼36% during the dry season, followed by Bolivia (∼28% annually, ∼29% in the dry season). Most of this moisture returns to forested areas within these countries, in proportion significantly higher than their forest cover (Figure 8a). For example, while Peru is 57% forested (52% selected rainforest), over 80% of the Amazon-rainforest-sourced precipitation falls on this land-use type. Brazil, despite having about 58% forest cover (including 35% selected rainforest) and hosting the largest share of the Amazon rainforest, relies on recycled moisture for only ∼11% of its rainfall. All downwind countries show increased dependence on Amazon moisture during the dry season, with the largest absolute increase in Ecuador, from ∼25% to ∼33% of its total precipitation (Figure 7a). In addition, Ecuador's annual dependence on rainforest moisture strongly correlates with increasing rainforest dryness. All statistically significant correlations (p-value <0.05) show increased dependence on Amazon moisture with increased dryness; this includes Ecuador, Colombia, Peru, and Paraguay.

Similar trends are found in the countries downwind of the Congo rainforest (Figure 7b). The countries most reliant on moisture recycling from the Congo are located to the west of the forest, namely Gabon (∼25%), Congo (∼23%), and Equatorial Guinea (∼22%). As shown in Figure 8b, the forested areas (including non-rainforest types and rainforest outside of the selection area) in most countries receive rainfall from the Congo rainforest in proportions that exceed their forest cover. We find that countries south of the Congo rainforest, such as Angola, Zambia, and southern DRC, depend more on Congo rainforest moisture during the JF season, with Angola and Zambia nearly doubling their dependence (Figure 7b) which is in agreement with the patterns shown in Figures 4d and 4f. In contrast, countries north of the rainforest, such as Nigeria, CAR, Cameroon, and South Sudan, have

19447973, 2026, 9, Downloaded from https://agupubs.onlinelibrary.wiley.com/doi/10.1029/2025WR043039 by Technical University Delft, Wiley Online Library on [10/09/2026]. See the Terms and Conditions (https://onlinelibrary.wiley.com/terms-and-conditions) on Wiley Online Library for rules of use; OA articles are governed by the applicable Creative Commons License

10.1029/2025WR043039

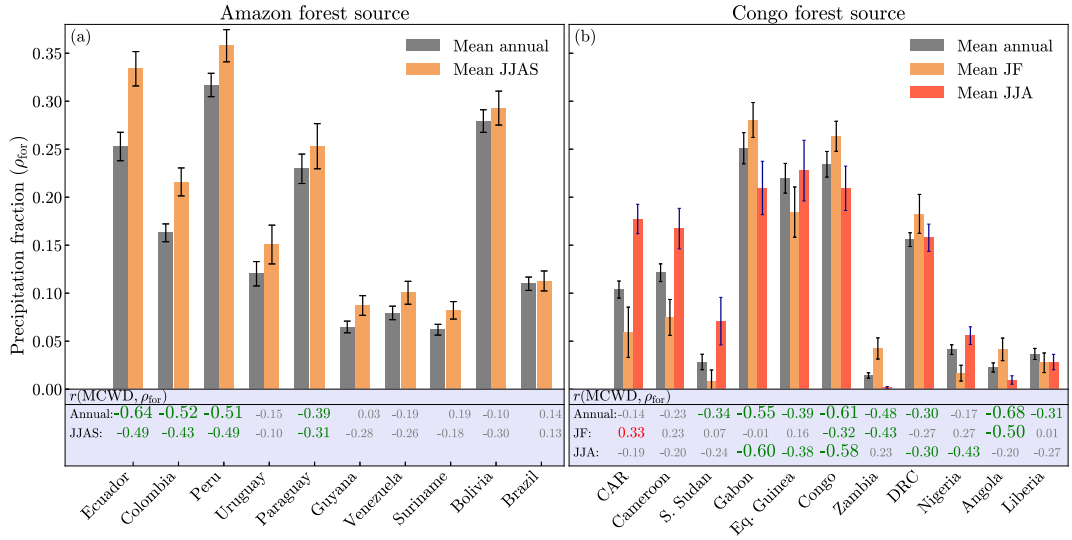


Figure 7. Precipitation fraction (ρ_{for}) originating from the Amazon (a) and Congo (b) rainforests to selected downstream countries (*x*-axes). Gray bars show annual means over the period 1980–2023. Dry season means are shown in orange (Amazon: JJAS; Congo: JF) and red (Congo: JJA). Error bars indicate one standard deviation of inter-annual variability. Correlations between rainforest dryness and precipitation dependence on rainforest moisture are shown below each panel: green values indicate increasing dependence with increasing dryness ($r(\text{MCWD}, \rho_{for}) < 0$), red values indicate decreasing dependence ($r > 0$), and gray values denote non-significant correlations (p-values ≥ 0.5). Correlations above 0.5 or below −0.5 are printed in a larger font. CAR stands for the Central African Republic, and DRC stands for the Democratic Republic of Congo. Countries are ordered by decreasing difference in precipitation fraction between the mean annual and the dry season.

higher dependence during the JJA season. Further along the West African coast, Liberia receives less moisture from the rainforest in both dry seasons, which is also reflected in the slight red anomalies in Figure 4 during both seasons in that region. Within the rainforest, dependence patterns also align with Figures 4d and 4f: Congo and Gabon, located further south, receive more rainforest rainfall during the JF season, whereas the more northerly Equatorial Guinea shows greater dependence during JJA.

Amplification trends are strongest near the western edge of the Congo rainforest (Figure 7b). The Republic of Congo shows an amplified dependence on rainforest-sourced rainfall during both dry seasons. Even Liberia, which generally depends less on rainforest moisture during dry seasons, shows increased dependence during exceptionally dry years. The only significant exception is the Central African Republic, which shows reduced dependence on rainforest-sourced moisture during increasingly dry JF seasons.

Using MSWEP precipitation fields to run WAM2layers (Figure S11 in Supporting Information S1) results in higher annual and dry-season dependence on Amazon moisture for several countries: Ecuador (+4%, +4% percentage points for annual and dry-season, respectively), Colombia (+1%, +1%), Peru (+6%, +6%), Uruguay (+2%, +2%), Paraguay (+3%, +3%), and Bolivia (+5%, +7%). Slightly lower dependencies ($\leq -1\%$) are found for Suriname, Guyana, Venezuela, and Brazil. In Africa, differences between the MSWEP and ERA5-based estimates are no larger than one percentage point, with the exception of Equatorial Guinea during JJA-season (+3%). Most significant correlations with dryness disappear in South America when using MSWEP, but they remain overall consistent in Africa.

7. Discussion

7.1. Comparing Moisture Recycling in the Amazon and Congo Rainforests

Although the Amazon and Congo rainforests differ significantly in their seasonal cycles of precipitation, evaporation, and moisture recycling ratios (see Figure 2), meaningful parallels can be drawn between their moisture recycling systems. In both forests, seasonal shifts in the ITCZ strongly influence moisture recycling dynamics, albeit in different ways. These shifts affect both the location of moisture sources and the regions where recycled moisture from the forests precipitates (see Figures 3 and 4). Importantly, our focus is on the origin and transport of

19447973, 2026, 9, Downloaded from https://agupubs.onlinelibrary.wiley.com/doi/10.1029/2025WR043039 by Technical University Delft, Wiley Online Library on [10/09/2026]. See the Terms and Conditions (https://onlinelibrary.wiley.com/terms-and-conditions) on Wiley Online Library for rules of use; OA articles are governed by the applicable Creative Commons License

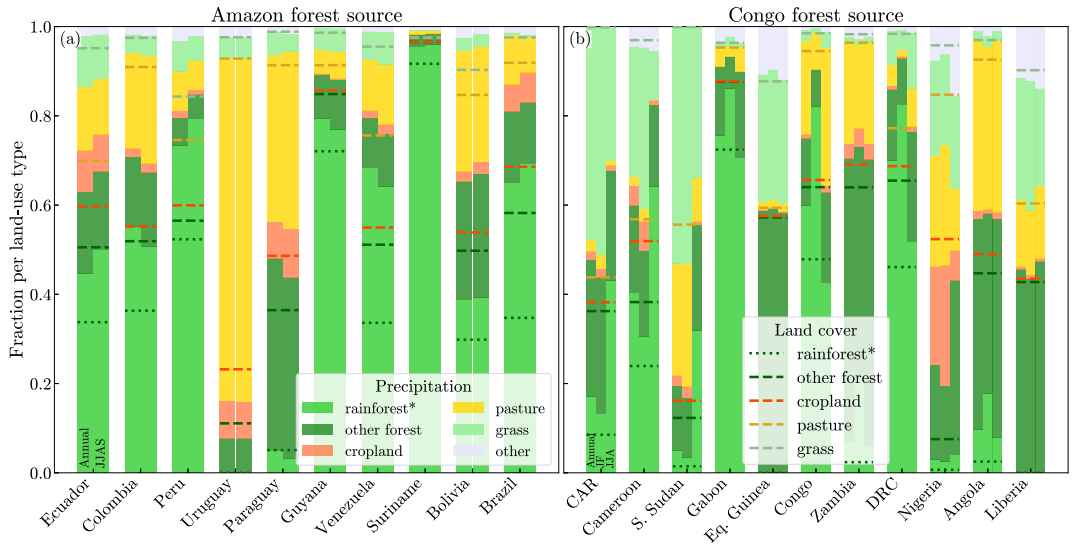


Figure 8. Precipitation fractions by land-use type originating from the Amazon (a) and Congo (b) forests and falling on selected downstream countries (*x*-axes). Green bars indicate precipitation falling on all forest types (incl. non-rainforest types), coral on cropland, yellow on pastures, light green on grasslands, and gray on other surfaces, including water bodies. For each country, the left bars represent annual means and the right (Amazon) or middle and right (Congo) bars represent dry-season means for the time-varying land-mask restricted period of 1980–2019. Dashed lines show the corresponding land-cover fractions of selected rainforest (bright green), all other forest (dark green), cropland (red), pasture (yellow), and grassland (light green). CAR denotes the Central African Republic, and DRC the Democratic Republic of the Congo.

moisture, rather than on local-scale processes of rainfall generation. e.g., recent work indicates that rainfall variability in the Congo rainforest may also strongly depend on how moisture is organized and converges within the atmosphere (e.g., Longandjo & Rouault, 2024).

Moisture flow anomalies from oceanic sources are primarily driven by circulation shifts, whereas moisture recycling within the rainforests is more closely tied to local processes, with varying sensitivity on the dryness index (see Figure 5). During the dry season (only JJA for Congo), both rainforests show a slight but statistically significant increase in dependence on internally recycled moisture (see Tables 1 and 2). Most surrounding downwind countries also become more reliant on moisture recycled from the rainforests during the dry seasons (incl. JF Congo) (Figure 7), and this reliance disproportionally involves forest covered areas (Figure 8). Additionally, moisture flows recycled from forests outside of the selected rainforest areas remain more stable than those from other land-use types (see Figure 6).

7.2. Literature Comparison

Generally, our findings of annual average moisture recycling percentages within the rainforest are lower than those found in other studies, which is expected as our selected forest moisture source region is typically smaller than others' source region selections (see Tables 3 and 4). A comparison of the results with previous findings is challenging due to differences in definitions, such as forest area and study period. This matters because the efficacy of moisture recycling within forests is highly dependent on forest size: smaller areas offer less opportunity for evaporated moisture to return as precipitation. Consequently, comparing anomalies is more meaningful than comparing absolute averages across studies. To provide the most meaningful absolute comparison possible, we define an upper limit as the total moisture recycling from all land sources (Amazon: ∼35%, Congo: ∼55%), and a lower limit as the recycling occurring strictly within forested areas (included in the tables). Most of the earlier estimates fall between these two bounds. The range of dry-season anomalies reported in previous studies reflects these definitional differences: for the Amazon, our result (a relative increase of ∼5%) aligns with most earlier findings (4%–8%). For the Congo, the range of anomalies in the literature is considerable, with Baker and Spracklen (2022) reporting an increase of 7% at one extreme, and an increase of almost 40% at the other extreme, as reported by Dyer et al. (2017). Our analysis indicates an increase of approximately 12% in moisture recycling within the Congo rainforest during the JJA dry season.

19447973, 2026, 9, Downloaded from https://agupubs.onlinelibrary.wiley.com/doi/10.1029/2025WR043039 by Technical University Delft, Wiley Online Library on [10/09/2026]. See the Terms and Conditions (https://onlinelibrary.wiley.com/terms-and-conditions) on Wiley Online Library for rules of use; OA articles are governed by the applicable Creative Commons License

Table 3
Moisture Recycling in the Amazon Region or Selection Therein, Non-Exhaustive Overview of the Literature

Ref.	Annual (ρ_{for})	Dry season (ρ_{for})	Region	Time period and data	Method
Eltahir and Bras (1994)	25%	highest: ~28% (Jun), lowest: ~22% (Jan)	Amazon basin	1985–1990, ECMWF	2D recycling model
Burde et al. (2006)	31%	highest: 38% (Nov), lowest: 20% (June)	Box 4°N–16° S, 50° − 16°W	1981–1993, 2° × 2° monthly data from the Data Assimilation Office	2D recycling model
	26%	highest: 29% (Nov), lowest: 21% (June)			Budyko model
	41%	highest: 45% (Nov), lowest: 35% (June)			IMB model
	45%	highest: ~50% (Aug), lowest: ~38% (May)			Modified general model
Angelini et al. (2011)	25% from land	Higher recycling in dry season (not quantified)	Amazon basin	1999, sampling at three sites along Amazon river	Isotopic
Satyamurty et al. (2013)	–	37% in rainy season, 16% in dry season	Box 40°N–50° S, 20° − 120°W	1978–2010 NCEP/NCAR, 1986–2010 GPCC	Box model, based on moisture convergence
Bagley et al. (2014)	–	67.3% in dry season (JAS)	Box	2003–2010	Quasi-isentropic back trajectory, WRF
Zemp et al. (2014)	28%	30%	Amazon basin	2001–2010 TRMM + MODIS	WAM2layers
	24%	25%		1990–1995 LandFlux-EVAL and average of CRU, GPCC, GPCP and CPC	
Staal et al. (2018)	32%	–	Amazon basin	2003–2014, PCR-GLOBWB, ERA-I, CRU, LandFlux-EVAL	Lagranian moisture tracking
Baker and Spracklen (2022)	36.5 ± 4.9%	~37% in JJAS (Figure 3). Peak in SON: ~ 39%	Amazon basin	CMIP6 models	Recycling estimation method based on Eltahir and Bras (1994)
	36.2 ± 1.2%	~37% in JJAS (Figure 3). Peak in SON: ~41–42%		Reanalyses	
Yang and Dominguez (2019)	29.4%	32.9%	Amazon basin	2004–2013, WRF-WVT + Noah-MP + MODIS + ERA-I	WRF-WVT
Chug et al. (2022)	25%	25% in JJA, 26% in DJF	Box over Amazon basin	2003-2013, ERA-I	WRF-WVT
Claros et al. (2025)	26%	–	Amazon basin	2000–2021, convection-permitting model	2L-DRM
	25.6%	35%		2019, WRF-WVT convection-permitting model	WRF-WVT
This study	26%	28%	Amazon >85% rainforest	1980–2013, ERA-I, MSWEP	WAM2layers v.1
	21.3 ± 0.7%	22.3%		1980–2023, ERA5	WAM2layers v.3
	21.0 ± 0.7%	22.0%		1981–2017, ERA5 + MSWEP	

7.3. Uncertainty and Sensitivity

Our moisture recycling estimates using MSWEP and ERA5 precipitation are generally more consistent in the Congo rainforest than in the Amazon rainforest. The MSWEP simulation demonstrates a higher annual and dry-season dependence on Amazon moisture for most countries than the ERA5 simulation, while only minor discrepancies exist between the two over the Congo rainforest. When considering total area averages and air-footprint normalized anomalies, a general agreement is found between the two runs. However, the MSWEP simulation gives a consistently lower correlation between dryness and moisture recycling metrics. This may be associated with the discrepancy in ERA5 precipitation data, as identified by (Polasky et al., 2025).

A preprint of this work was released in 2022 (Wang-Erlandsson et al., 2023). The earlier research used ERA-Interim data with MSWEP precipitation fields as opposed to the ERA5 data used here. Some notable differences were found using the newer data set, which we believe are important to emphasize in order to demonstrate the sensitivity of our methods using different meteorological data. In this earlier version, moisture recycling

19447973, 2026, 9, Downloaded from https://agupubs.onlinelibrary.wiley.com/doi/10.1029/2025WR043039 by Technical University Delft, Wiley Online Library on [10/09/2026]. See the Terms and Conditions (https://onlinelibrary.wiley.com/terms-and-conditions) on Wiley Online Library for rules of use; OA articles are governed by the applicable Creative Commons License

19447973, 2026, 9, Downloaded from https://agupubs.onlinelibrary.wiley.com/doi/10.1029/2025WR043039 by Technical University Delft, Wiley Online Library on [10/09/2026]. See the Terms and Conditions (https://onlinelibrary.wiley.com/terms-and-conditions) on Wiley Online Library for rules of use; OA articles are governed by the applicable Creative Commons License

Table 4
Moisture Recycling in the Congo Region or Selection Therein, Non-Exhaustive Overview of the Literature

Ref.	Annual (ρ_{for})	Dry season (ρ_{for})	Region	Time period and data	Method
Pokam et al. (2012)	38 %	Feb: ~43%, JAS: 42%, lowest: ~33% (rainy season)	Box 5°N–5°S, 12.5°–30°E	1968–2000, 6h data NCEP reanalyses	2D recycling model
	–	highest: ~31% (Feb + Jul): 42%, lowest: ~24% (Nov)			Budyko type model of Brubaker et al. (1993)
	–	highest: ~48% (Feb + Jul): 42%, lowest: ~39% (Nov)			Tank model of Zangvil et al. (2004)
Dyer et al. (2017)	28%	JJA: 39%, DJF: 25%	Box over Congo Basin north: 2°N–5°S, 15°–30°E, and south: 2°–10°S, 15°–30°E	1980–2000	Water tagging ability in CESM1.2
Sorí et al. (2017)	59%	highest: ~65% (May), lowest: 55% (July)	Congo basin	1980–2010, P from CRU, ocean E from OAFlux, land E from GLEAM, moisture fluxes from ERA-I	Lagrangian model FLEXPART
te Wierik et al. (2022)	68%		Congo basin	1981–2016, ERA-I, MSWEP, GLEAM	Lagrangian model FLEXPART
Baker and Spracklen (2022)	41.9 ± 4.9%	JF: ~45%, JJA: ~40–50% (Figure 3)	Congo basin	CMIP6	Recycling estimation method based on Eltahir and Bras (1994)
	39.7 ± 3.1%	JF: ~45%, JJA: ~45% (Figure 3)		Reanalyses	
This study	28%	JF: 28%, JJA: 36%	Africa where >85% rainforest	1980–2013, ERA-I, MSWEP	WAM2layers v.1
	23.7 ± 0.7%	JF: 24.1%, JJA: 26.7%		1980–2023, ERA5	WAM2layers v.3
	24.2 ± 0.8%	JF: 23.9%, JJA: 28.2%		1981–2017, ERA5 + MSWEP	

within the rainforest was found to be higher, at 26% in the Amazon and 28% in the Congo. The dry-season anomaly was relatively similar to what we find now in the Amazon, and larger in the Congo area, with a 21% increase instead of the 12% found here. Large differences are observed between the moisture source regions for the Amazon, where the discernible signal from the Tropical Atlantic, visible in Figure 3a, is absent from the ERA-Interim results. Both dry season precipitation anomalies in Congo (Figure 4) exhibit a more northward orientation than was observed in the ERA-Interim result. This results in some changes in the precipitation dependence of downwind countries. For example, the preprint suggested a high JJA dry season dependence of precipitation from rainforest moisture in Congo and Gabon of up to approx. 50%, whereas this study shows that the dependence is lower than the mean annual at approx. 20%. The observed discrepancies can be primarily attributed to differences within the wind fields and evaporation fields, since these differences are not evident between our ERA5 and MSWEP precipitation runs. The preprint found significant amplifications in ρ_{for} with increasing drought index, whereas we did not observe such a pattern (see top row last two values of Table 1 and last three values of Table 2). Nonetheless, we do find amplifications in countries' dependence on rainforest-sourced moisture under increasing dryness. In most cases, the proportions of rainfall originating from rainforests that falls on all forested areas (including rainforest outside of the selected area and non-rainforest types) exceeds the total forest cover (see Figure 8, suggesting that while local rainforest recycling may not intensify, the broader reliance on rainforest moisture does. Readers interested in further details regarding the discrepancies between the ERA-Interim and ERA5 simulation results are encouraged to consult the preprint.

7.4. Potential Implications for Forest Governance

Increasingly, policies to promote nature-based solutions to address climate change such as forest restoration and conservation are being proposed, planned and implemented (Chaplin-Kramer et al., 2019; Griscom et al., 2017). The benefit of forest moisture supply for forest resilience, agriculture, and water resources are increasingly recognized (Cui et al., 2022; Hoek van Dijke et al., 2022; Leite-Filho et al., 2021). At the same time, dry season length in both the Amazon and Congo forests is increasing (Fu et al., 2013; Jiang et al., 2019) and rainforests are

19447973, 2026, 9, Downloaded from https://agupubs.onlinelibrary.wiley.com/doi/10.1029/2025WR043039 by Technical University Delft, Wiley Online Library on [10/09/2026]. See the Terms and Conditions (https://onlinelibrary.wiley.com/terms-and-conditions) on Wiley Online Library for rules of use; OA articles are governed by the applicable Creative Commons License

becoming increasingly vulnerable to repeated droughts (Tao et al., 2022). Thus, it will be important to understand where measures to prevent deforestation or promote forestation might have the greatest benefits for counteracting such drying trends (Tuinenburg et al., 2022). More than 30% of the moisture that precipitates in the Congo rainforest originates from land outside of the rainforest, much higher than the dependence on evaporation from the rainforest itself (∼24%), indicating that substantial land areas without dense forests are also important for moisture supply to rainfall. The same applies to the Amazon, though to a lesser extent. Compared to the Amazon, the Congo rainforest is also projected to face greater future threats of forest loss and greater impacts of deforestation on regional precipitation (Smith et al., 2023).

The need for governance of moisture flows is increasingly being discussed in the scientific literature (Keys et al., 2017; te Wierik et al., 2020). Hitherto, most analyses of moisture flows at the country scale focus on the mean annual scale (Dirmeyer et al., 2009; Keys et al., 2017). However, Figures 7 and 8 reveal substantial seasonal variations in both the forest's contribution to rainfall and the spatial distribution of where this rain occurs. For example, in South Sudan, the reliance on forest-sourced moisture increases from negligible (∼1%) in January and February to substantial (∼7%) in June, July, and August. Concurrently, while only about 20% of this rainfall returns to the forested areas of South Sudan, more than 55% does so during the summer months. This means that considering the importance of forests for different nations' management and governance contexts will need to go beyond the mean annual scale and account for seasonal variations.

As discussed in Section 7.2, the existing literature shows a wide range of results, particularly in the Congo region. In addition, results are sensitive to the use of different data set, as shown in Section 7.3. This highlights the critical need to improve data availability to support policy development and enable a more accurate understanding and quantification of uncertainty. Therefore, it is vital to increase data availability for policy for better understanding and quantification of uncertainty. At the same time, policy design must be responsive to present uncertainties, aiming to generate benefits while minimizing the risks when accounting for moisture recycling in management and governance frameworks.

8. Conclusion

In this study, we quantified moisture recycling in both the Amazon and Congo rainforests during 1980–2023, and studied both the sources and sinks of the recycled water during the dry season and drought years. We draw the following conclusions:

- On average, between 1980 and 2023, 21.3 ± 0.7% of the annual precipitation in the Amazon rainforest and 23.7 ± 0.7% in the Congo rainforest depend on moisture recycling within the rainforests themselves. 41 ± 2% and 32 ± 4% of all evaporation is rained down back into the Amazon and Congo rainforests, respectively.
- Both the Congo and Amazon rainforests become significantly (>1σ) more reliant on their own moisture supply during the dry season: +1 percentage points (increase of 5%) during JJAS in the Amazon, and +3 percentage points (increase of 12%) during JJA in the Congo. No significant increase in moisture self-reliance is found for the JF Congo dry season. However, a larger fraction of its evaporation leaves the rainforest: +9 percentage points (increase of 15%) for JJAS in the Amazon, and +7 percentage points (increase of 10%) for JF in the Congo. No significant difference is found for the JJA Congo dry season. Strong correlations between all seasons and regions, and the drought index MCWD indicate that during drier years, the fraction of evaporation that leaves the rainforest becomes more pronounced.
- Correlations between dry-season air-mass footprint anomalies and moisture source anomalies reveal that oceanic sources are strongly influenced by air-mass transport, while rainforest sources are more locally controlled. For the Amazon rainforest, the relationship between anomalies in air-mass footprint and moisture sources shifts with dryness, becoming even anti-correlated in dry years for terrestrial moisture sources. For the Congo rainforest, circulation shifts are the main driver of land moisture source anomalies outside the rainforest and decrease in importance with increasing dryness. No significant correlation is found between dryness and the importance of circulation shifts as a driver of oceanic moisture sources to the Congo rainforest.
- Different land-use types vary in their ability to buffer moisture supply to the rainforests during dry seasons: in the Amazon, forest-type sources (excl. The selected rainforest) show the smallest reduction in moisture contribution compared to the annual mean (−37%: E_{for}/f_{air} is 37% smaller for JJAS than the annual mean), while cropland (−55%), pasture (−38%), and grassland (−55%) show (slightly) weaker buffering. In the

Congo, seasonal shifts in air-mass paths lead to variable buffering, with grasslands contributing slightly more during the JJA dry season (−4%), but much less during JF season (−28%).

- At the country scale in South America, Peru is the country that relies most on rainforest moisture for its rainfall, receiving 36% of its dry season rainfall from rainforest moisture. Ecuador sees the largest seasonal increase, from 25% annually to 33% in the dry season. Significant positive correlations between forest dryness and dependence are observed in Ecuador, Colombia, Peru, and Paraguay. In Africa, Gabon (25%), Congo (23%), and Equatorial Guinea (22%) depend most on forest-sourced rainfall. The largest seasonal difference is found in the Central African Republic. Seasonal patterns align with wind shifts: southern countries like Angola and Zambia nearly double their Congo moisture dependence during JF, while northern countries like Nigeria and Cameroon are more dependent during JJA. Amplification of dependence with dryness is strongest south and west of the rainforest.
- In most countries, the proportion of rainforest-sourced moisture precipitating on forested areas exceeds their total forest cover, indicating a disproportionate reliance on forests for moisture recycling.

Conflict of Interest

The authors declare no conflicts of interest relevant to this study.

Availability Statement

Processed data and scripts used for the creation of all results can be found at Bakels, Wang-Erlandsson, et al. (2025).

Acknowledgments

We would like to thank Carlos Nobre, Francina Dominguez, and the three anonymous reviewers for their helpful comments. We would also like to thank Prof. Hubert Savenije for valuable discussions during research design and useful comments on the manuscript. We acknowledge support from the Svenska Forskningsrådet Formas (the projects "SAFER" 2022-02089, "ReForMit" 2023-00321 and "ESI" 2023-00310) and from the Swedish Research Council (Project "Beyond Forest-Rainfall myths", 2014-1224). LWE further acknowledges funding from the Japan Society for the Promotion of Science (JSPS) postdoctoral fellowship (ID: P-17761), and the IKEA Foundation. We thank the PDC Center for High Performance Computing, KTH Royal Institute of Technology, Sweden, for providing access to the computing resources used in this research. The computations were enabled by resources provided by the National Academic Infrastructure for Supercomputing in Sweden (NAISS), partially funded by the Swedish Research Council through Grant agreement 2022-06725. In addition, we acknowledge various public Python packages that have benefited our study: NumPy (Harris et al., 2020), Matplotlib (Hunter, 2007), Xarray (Hoyer & Hamman, 2017), and cartopy (Met Office, 2010–2015).

References

Angelini, I. M., Garstang, M., Davis, R. E., Hayden, B., Fitzjarrald, D. R., Legates, D. R., et al. (2011). On the coupling between vegetation and the atmosphere. *Theoretical and Applied Climatology*, *105*(1–2), 243–261. https://doi.org/10.1007/s00704-010-0377-5

Bagley, J. E., Desai, A. R., Harding, K. J., Snyder, P. K., & Foley, J. A. (2014). Drought and deforestation: Has land cover change influenced recent precipitation extremes in the Amazon? *Journal of Climate*, *27*(1), 345–361. https://doi.org/10.1175/jcli-d-12-00369.1

Bakels, L., Blaschek, M., Dütsch, M., Plach, A., Lechner, V., Brack, G., et al. (2025). LARA: A lagrangian reanalysis based on ERA5 spanning from 1940 to 2023. *Earth System Science Data*, *17*(9), 4569–4585. https://doi.org/10.5194/essd-17-4569-2025

Bakels, L., Tatsii, D., Tipka, A., Thompson, R., Dütsch, M., Blaschek, M., et al. (2024). FLEXPART version 11: Improved accuracy, efficiency, and flexibility. *Geoscientific Model Development*, *17*(21), 7595–7627. https://doi.org/10.5194/gmd-17-7595-2024

Bakels, L., Wang-Erlandsson, L., van der Ent, R., Staal, A., Keys, P., Zemp, D. C., et al. (2025). Amazon and Congo rainforest moisture recycling [Dataset]. https://doi.org/10.5281/zenodo.17752136

Baker, J. C. A., & Spracklen, D. V. (2022). Divergent representation of precipitation recycling in the Amazon and the Congo in CMIP6 models. *Geophysical Research Letters*, *49*(10), e2021GL095136. https://doi.org/10.1029/2021GL095136

Baudena, M., Tuinenburg, O. A., Ferdinand, P. A., & Staal, A. (2021). Effects of land-use change in the Amazon on precipitation are likely underestimated. *Global Change Biology*, *27*(21), 5580–5587. https://doi.org/10.1111/gcb.15810

Beck, H. E., Wood, E. F., Pan, M., Fisher, C. K., Miralles, D. G., van Dijk, A. I. J. M., et al. (2019). MSWEP v2 global 3-hourly 0.1° precipitation: Methodology and quantitative assessment. *Bulletin of the American Meteorological Society*, *100*(3), 473–500. https://doi.org/10.1175/BAMS-D-17-0138.1

Benedict, I., Keune, J., Weijenborg, C., van der Ent, R., Kalverla, P., Koren, G., et al. (2026). Identification of sources of precipitation through an international research effort (inspire): Three extreme precipitation case studies. *Bulletin of the American Meteorological Society, BAMS-D-25-0057.1*. https://doi.org/10.1175/BAMS-D-25-0057.1

Benedict, I., van Heerwaarden, C. C., van der Linden, E. C., Weerts, A. H., & Hazeleger, W. (2021). Anomalous moisture sources of the Rhine basin during the extremely dry summers of 2003 and 2018. *Weather and Climate Extremes*, *31*, 100302. https://doi.org/10.1016/j.wace.2020.100302

Brubaker, K. L., Entekhabi, D., & Eagleson, P. S. (1993). Estimation of Continental precipitation recycling. *Journal of Climate*, *6*(6), 1077–1089. https://doi.org/10.1175/1520-0442(1993)006<1077:eocpr>2.0.co;2

Burde, G. I., Gandush, C., & Bayarjargal, Y. (2006). Bulk recycling models with incomplete vertical mixing. Part ii: Precipitation recycling in the Amazon basin. *Journal of Climate*, *19*(8), 1473–1489. https://doi.org/10.1175/JCLI3688.1

Chaplin-Kramer, R., Sharp, R. P., Weil, C., Bennett, E. M., Pascual, U., Arkema, K. K., et al. (2019). Global modeling of nature's contributions to people. *Science*, *366*(6462), 255–258. https://doi.org/10.1126/science.aaw3372

Chug, D., Dominguez, F., & Yang, Z. (2022). The Amazon and La Plata river basins as moisture sources of South America: Climatology and intraseasonal variability. *Journal of Geophysical Research: Atmospheres*, *127*(12), e2021JD035455. https://doi.org/10.1029/2021JD035455

Claros, E., Dominguez, F., & Liu, C. (2025). Moisture sources of precipitation using convection-permitting simulations: A study over South america. *Geophysical Research Letters*, *52*(23), e2025GL118806. https://doi.org/10.1029/2025GL118806

Costa, M. H., Biajoli, M. C., Sanches, L., Malhado, A. C. M., Hutyra, L. R., da Rocha, H. R., et al. (2010). Atmospheric versus vegetation controls of Amazonian tropical rain forest evapotranspiration: Are the wet and seasonally dry rain forests any different? *Journal of Geophysical Research*, *115*(G4). https://doi.org/10.1029/2009jg001179

Costa, M. H., Borma, L., Brando, P. M., Marengo, J. A., Saleska, S. R., & Gatti, L. V. (2021). Chapter 7: Biogeophysical cycles: Water recycling, climate regulation. In C. Nobre, A. Encalada, E. Anderson, F. H. Roca Alcazar, M. Bustamante, C. Mena, et al. (Eds.), *Amazon assessment report 2021*. United Nations Sustainable Development Solutions Network. https://doi.org/10.55161/KKHX1998

19447973, 2026, 9, Downloaded from https://agupubs.onlinelibrary.wiley.com/doi/10.1029/2025WR043039 by Technical University Delft, Wiley Online Library on [10/09/2026]. See the Terms and Conditions (https://onlinelibrary.wiley.com/terms-and-conditions) on Wiley Online Library for rules of use; OA articles are governed by the applicable Creative Commons License

Crockford, R., & Richardson, D. (2000). Partitioning of rainfall into throughfall, stemflow and interception: Effect of forest type, ground cover and climate. *Hydrological Processes*, *14*(16–17), 2903–2920. https://doi.org/10.1002/1099-1085(200011/12)14:16/17<2903::aid-hyp126>3.0.co;2-6

Cui, J., Lian, X., Huntingford, C., Gimeno, L., Wang, T., Ding, J., et al. (2022). Global water availability boosted by vegetation-driven changes in atmospheric moisture transport. *Nature Geoscience*, *15*(12), 982–988. https://doi.org/10.1038/s41561-022-01061-7

Dirmeyer, P. A., Brubaker, K. L., & DelSole, T. (2009). Import and export of atmospheric water vapor between nations. *Journal of Hydrology*, *365*(1), 11–22. https://doi.org/10.1016/j.jhydrol.2008.11.016

Dominguez, F., Eiras-Barca, J., Yang, Z., Bock, D., Nieto, R., & Gimeno, L. (2022). Amazonian moisture recycling revisited using WRF with water vapor tracers. *Journal of Geophysical Research: Atmospheres*, *127*(4), e2021JD035259. https://doi.org/10.1029/2021JD035259

do Nascimento, M. G., Herdies, D. L., & de Souza, D. O. (2016). The South American water balance: The influence of low-level jets. *Journal of Climate*, *29*(4), 1429–1449. https://doi.org/10.1175/JCLI-D-15-0065.1

Dyer, E. L. E., Jones, D. B. A., Nusbaumer, J., Li, H., Collins, O., Vettoretti, G., & Noone, D. (2017). Congo Basin precipitation: Assessing seasonality, regional interactions, and sources of moisture. *Journal of Geophysical Research: Atmospheres*, *122*(13), 6882–6898. https://doi.org/10.1002/2016jd026240

Eamus, D., Huete, A., & Yu, Q. (2016). Seasonal behaviour of vegetation of the Amazon basin. In *Vegetation dynamics: A synthesis of plant ecophysiology, remote sensing and modelling* (pp. 415–441). Cambridge University Press.

Eltahir, E. A. B., & Bras, R. L. (1994). Precipitation recycling in the Amazon basin. *Quarterly Journal of the Royal Meteorological Society*, *120*(518), 861–880. https://doi.org/10.1002/qj.49712051806

Fu, R., Yin, L., Li, W., Arias, P. A., Dickinson, R. E., Huang, L., et al. (2013). Increased dry-season length over southern Amazonia in recent decades and its implication for future climate projection. *Proceedings of the National Academy of Sciences*, *110*(45), 18110–18115. https://doi.org/10.1073/pnas.1302584110

Garreaud, R. D., Vuille, M., Compagnucci, R., & Marengo, J. (2009). Present-day South American climate. *Palaeogeography, Palaeoclimatology, Palaeoecology*, *281*(3), 180–195. https://doi.org/10.1016/j.palaeo.2007.10.032

Gash, J. H. C. (1979). An analytical model of rainfall interception by forests. *Quarterly Journal of the Royal Meteorological Society*, *105*(443), 43–55. https://doi.org/10.1002/qj.49710544304

Gerrits, A. M. J., Pfister, L., & Savenije, H. H. G. (2010). Spatial and temporal variability of canopy and forest floor interception in a beech forest. *Hydrological Processes*, *24*(21), 3011–3025. https://doi.org/10.1002/hyp.7712

Griscom, B. W., Adams, J., Ellis, P. W., Houghton, R. A., Lomax, G., Miteva, D. A., et al. (2017). Natural climate solutions. *Proceedings of the National Academy of Sciences*, *114*(44), 11645–11650. https://doi.org/10.1073/pnas.1710465114

Harris, C. R., Millman, K. J., van der Walt, S. J., Gommers, R., Virtanen, P., Cournapeau, D., et al. (2020). Array programming with NumPy. *Nature*, *585*(7825), 357–362. https://doi.org/10.1038/s41586-020-2649-2

Hauser, M., Spring, A., Busecke, J., van Driel, M., & Lorenz, R. (2024). Regionmask/regionmask: Version 0.12.1. *Zenodo*. https://doi.org/10.5281/zenodo.10849860

Hersbach, H., Bell, B., Berrisford, P., Hirahara, S., Horányi, A., Muñoz-Sabater, J., et al. (2020). The ERA5 global reanalysis. *Quarterly Journal of the Royal Meteorological Society*, *146*(730), 1999–2049. https://doi.org/10.1002/qj.3803

Hoek van Dijke, A. J., Herold, M., Mallick, K., Benedict, I., Machwitz, M., Schlerf, M., et al. (2022). Shifts in regional water availability due to global tree restoration. *Nature Geoscience*, *15*(5), 363–368. https://doi.org/10.1038/s41561-022-00935-0

Horel, J. D., Hahmann, A. N., & Geisler, J. E. (1989). An investigation of the annual cycle of convective activity over the tropical Americas. *Journal of Climate*, *2*(11), 1388–1403. https://doi.org/10.1175/1520-0442(1989)002<1388:aiotac>2.0.co;2

Hoyer, S., & Hamman, J. (2017). Xarray: N-D labeled arrays and datasets in Python. *Journal of Open Research Software*, *5*(1), 10. https://doi.org/10.5334/jors.148

Hoyos, I., Dominguez, F., Cañón-Barriga, J., Martínez, J., Nieto, R., Gimeno, L., & Dirmeyer, P. (2018). Moisture origin and transport processes in Colombia, northern South America. *Climate Dynamics*, *50*(3), 971–990. https://doi.org/10.1007/s00382-017-3653-6

Hubau, W., Lewis, S. L., Phillips, O. L., Affum-Baffoe, K., Beeckman, H., Cuní-Sanchez, A., et al. (2020). Asynchronous carbon sink saturation in African and Amazonian tropical forests. *Nature*, *579*(7797), 80–87. https://doi.org/10.1038/s41586-020-2035-0

Hunter, J. D. (2007). Matplotlib: A 2d graphics environment. *Computing in Science & Engineering*, *9*(3), 90–95. https://doi.org/10.1109/MCSE.2007.55

Jiang, Y., Zhou, L., Tucker, C. J., Raghavendra, A., Hua, W., Liu, Y. Y., & Joiner, J. (2019). Widespread increase of boreal summer dry season length over the Congo rainforest. *Nature Climate Change*, *9*(8), 617–622. https://doi.org/10.1038/s41558-019-0512-y

Kalverla, P., Benedict, I., Weijenborg, C., & van der Ent, R. J. (2025). Atmospheric moisture tracking with WAM2layers v3. *Geoscientific Model Development*, *18*(14), 4335–4352. https://doi.org/10.5194/gmd-18-4335-2025

Keys, P. W., Barnes, E. A., van der Ent, R. J., & Gordon, L. J. (2014). Variability of moisture recycling using a precipitationshed framework. *Hydrology and Earth System Sciences*, *18*(10), 3937–3950. https://doi.org/10.5194/hess-18-3937-2014

Keys, P. W., Wang-Erlandsson, L., Gordon, L. J., Galaz, V., & Ebbesson, J. (2017). Approaching moisture recycling governance. *Global Environmental Change*, *45*, 15–23. https://doi.org/10.1016/j.gloenvcha.2017.04.007

Leite-Filho, A. T., Soares-Filho, B. S., Davis, J. L., Abrahão, G. M., & Börner, J. (2021). Deforestation reduces rainfall and agricultural revenues in the Brazilian Amazon. *Nature Communications*, *12*(1), 2591. https://doi.org/10.1038/s41467-021-22840-7

Lewis, S. L., Edwards, D. P., & Galbraith, D. (2015). Increasing human dominance of tropical forests. *Science*, *349*(6250), 827–832. https://doi.org/10.1126/science.aaa9932

Link, A., van der Ent, R., Berger, M., Eisner, S., & Finkbeiner, M. (2020). The fate of land evaporation – A global dataset. *Earth System Science Data*, *12*(3), 1897–1912. https://doi.org/10.5194/essd-12-1897-2020

Longandjo, G.-N. T., & Rouault, M. (2024). Revisiting the seasonal cycle of rainfall over central Africa. *Journal of Climate*, *37*(3), 1015–1032. https://doi.org/10.1175/JCLI-D-23-0281.1

Malhi, Y., Aragão, L. E. O. C., Galbraith, D., Huntingford, C., Fisher, R., Zelazowski, P., et al. (2009). Exploring the likelihood and mechanism of a climate-change-induced dieback of the Amazon rainforest. *Proceedings of the National Academy of Sciences*, *106*(49), 20610–20615. https://doi.org/10.1073/pnas.0804619106

Marengo, J. A., Cunha, A. P., Espinoza, J.-C., Fu, R., Schöngart, J., Jimenez, J. C., et al. (2024). The drought of Amazonia in 2023-2024. *American Journal of Climate Change*, *13*(3), 567–597. https://doi.org/10.4236/ajcc.2024.133026

Marengo, J. A., Tomasella, J., Alves, L. M., Soares, W. R., & Rodriguez, D. A. (2011). The drought of 2010 in the context of historical droughts in the Amazon region. *Geophysical Research Letters*, *38*(12). https://doi.org/10.1029/2011GL047436

19447973, 2026, 9, Downloaded from https://agupubs.onlinelibrary.wiley.com/doi/10.1029/2025WR043039 by Technical University Delft, Wiley Online Library on [10/09/2026]. See the Terms and Conditions (https://onlinelibrary.wiley.com/terms-and-conditions) on Wiley Online Library for rules of use; OA articles are governed by the applicable Creative Commons License

Met Office. (2010–2015). Cartopy: A cartographic python library with a matplotlib interface [Computer software manual]. *Exeter, Devon*. Retrieved from https://scitools.org.uk/cartopy

Miralles, D. G., Brutsaert, W., Dolman, A. J., & Gash, J. H. (2020). On the use of the term "evapotranspiration". *Water Resources Research*, *56*(11), e2020WR028055. https://doi.org/10.1029/2020WR028055

Mitchard, E. T. (2018). The tropical forest carbon cycle and climate change. *Nature*, *559*(7715), 527–534. https://doi.org/10.1038/s41586-018-0300-2

Mu, Y., Biggs, T. W., & Jones, C. (2023). Importance in shifting circulation patterns for dry season moisture sources in the Brazilian Amazon. *Geophysical Research Letters*, *50*(9), e2023GL103167. https://doi.org/10.1029/2023GL103167

Nicholson, S. E., & Klotter, D. A. (2021). Assessing the reliability of satellite and reanalysis estimates of rainfall in equatorial Africa. *Remote Sensing*, *13*(18), 3609. https://doi.org/10.3390/rs13183609

O'Connor, J. C., Dekker, S. C., Staal, A., Tuinenburg, O. A., Rebel, K. T., & Santos, M. J. (2021). Forests buffer against variations in precipitation. *Global Change Biology*, *27*(19), 4686–4696. https://doi.org/10.1111/gcb.15763

Pimm, S. L., Jenkins, C. N., Abell, R., Brooks, T. M., Gittleman, J. L., Joppa, L. N., et al. (2014). The biodiversity of species and their rates of extinction, distribution, and protection. *Science*, *344*(6187), 1246752. https://doi.org/10.1126/science.1246752

Pokam, W. M., Djiotang, L. A. T., & Mkankam, F. K. (2012). Atmospheric water vapor transport and recycling in equatorial Central Africa through NCEP/NCAR reanalysis data. *Climate Dynamics*, *38*(9–10), 1715–1729. https://doi.org/10.1007/s00382-011-1242-7

Polasky, A., Sapkota, V., Forest, C. E., & Fuentes, J. D. (2025). Discrepancies in precipitation trends between observational and reanalysis datasets in the Amazon basin. *Scientific Reports*, *15*(1), 7268. https://doi.org/10.1038/s41598-025-87418-5

Pypker, T. G., Unsworth, M. H., & Bond, B. J. (2006). The role of epiphytes in rainfall interception by forests in the Pacific Northwest. I. Laboratory measurements of water storage. *Canadian Journal of Forest Research*, *36*(4), 809–818. https://doi.org/10.1139/x05-298

Salati, E., Dall'Olio, A., Matsui, E., & Gat, J. R. (1979). Recycling of water in the Amazon basin: An isotopic study. *Water Resources Research*, *15*(5), 1250–1258. https://doi.org/10.1029/WR015i005p01250

Satyamurty, P., da Costa, C. P. W., & Manzi, A. O. (2013). Moisture source for the Amazon basin: A study of contrasting years. *Theoretical and Applied Climatology*, *111*(1–2), 195–209. https://doi.org/10.1007/s00704-012-0637-7

Schilperoort, B., Liu, Y., Doore, K., Levang, S., & Mares, B. (2024). xarray-regrid. Retrieved from https://github.com/EXCITED-CO2/xarray-regrid

Singh, C., van der Ent, R., Wang-Erlandsson, L., & Fetzer, I. (2022). Hydroclimatic adaptation critical to the resilience of tropical forests. *Global Change Biology*, *28*(9), 2930–2939. https://doi.org/10.1111/gcb.16115

Smith, C., Baker, J., & Spracklen, D. (2023). Tropical deforestation causes large reductions in observed precipitation. *Nature*, *615*(7951), 270–275. https://doi.org/10.1038/s41586-022-05690-1

Sorí, R., Nieto, R., Vicente-Serrano, S. M., Drumond, A., & Gimeno, L. (2017). A Lagrangian perspective of the hydrological cycle in the Congo river basin. *Earth System Dynamics*, *8*(3), 653–675. https://doi.org/10.5194/esd-8-653-2017

Spracklen, D. V., Arnold, S. R., & Taylor, C. (2012). Observations of increased tropical rainfall preceded by air passage over forests. *Nature*, *489*(7415), 282–285. https://doi.org/10.1038/nature11390

Staal, A., Tuinenburg, O. A., Bosmans, J. H., Holmgren, M., van Nes, E. H., Scheffer, M., et al. (2018). Forest-rainfall cascades buffer against drought across the Amazon. *Nature Climate Change*, *8*(6), 539–543. https://doi.org/10.1038/s41558-018-0177-y

Steinkopf, J., & Engelbrecht, F. (2022). Verification of ERA5 and ERA-interim precipitation over Africa at intra-annual and interannual timescales. *Atmospheric Research*, *280*, 106427. https://doi.org/10.1016/j.atmosres.2022.106427

Stohl, A., Hittenberger, M., & Wotawa, G. (1998). Validation of the lagrangian particle dispersion model FLEXPART against large-scale tracer experiment data. *Atmospheric Environment*, *32*(24), 4245–4264. https://doi.org/10.1016/S1352-2310(98)00184-8

Tao, S., Chave, J., Frison, P.-L., Toan, T. L., Ciais, P., Fang, J., et al. (2022). Increasing and widespread vulnerability of intact tropical rainforests to repeated droughts. *Proceedings of the National Academy of Sciences*, *119*(37), e2116626119. https://doi.org/10.1073/pnas.2116626119

te Wierik, S. A., Gupta, J., Cammeraat, E. L. H., & Artzy-Randrup, Y. A. (2020). The need for green and atmospheric water governance. *WIREs Water*, *7*(2), e1406. https://doi.org/10.1002/wat2.1406

te Wierik, S. A., Keune, J., Miralles, D. G., Gupta, J., Artzy-Randrup, Y. A., Gimeno, L., et al. (2022). The contribution of transpiration to precipitation over African watersheds. *Water Resources Research*, *58*(11), e2021WR031721. https://doi.org/10.1029/2021WR031721

Tuinenburg, O. A., Bosmans, J. H. C., & Staal, A. (2022). The global potential of forest restoration for drought mitigation. *Environmental Research Letters*, *17*(3), 034045. https://doi.org/10.1088/1748-9326/ac55b8

van der Ent, R. J., Savenije, H. H. G., Schaefli, B., & Steele-Dunne, S. C. (2010). Origin and fate of atmospheric moisture over continents. *Water Resources Research*, *46*(9). https://doi.org/10.1029/2010WR009127

van der Ent, R. J., Tuinenburg, O. A., Knoche, H.-R., Kunstmann, H., & Savenije, H. H. G. (2013). Should we use a simple or complex model for moisture recycling and atmospheric moisture tracking? *Hydrology and Earth System Sciences*, *17*(12), 4869–4884. https://doi.org/10.5194/hess-17-4869-2013

van der Ent, R. J., Wang-Erlandsson, L., Keys, P. W., & Savenije, H. H. G. (2014). Contrasting roles of interception and transpiration in the hydrological cycle part 2: Moisture recycling. *Earth System Dynamics*, *5*(2), 471–489. https://doi.org/10.5194/esd-5-471-2014

Wang-Erlandsson, L., van der Ent, R., Staal, A., Keys, P., Zemp, D. C., Fetzer, I., et al. (2023). *Dry periods amplify the Amazon and Congo forests' rainfall self-reliance*. ESS Open Archive. Retrieved from https://essopenarchive.org/users/308363/articles/632823-dry-periods-amplify-the-amazon-and-congo-forests-rainfall-self-reliancedoi:10.22541/essoar.168055170.04559257/v1

Winkler, K., Fuchs, R., Rounsevell, M., & Herold, M. (2021). Global land use changes are four times greater than previously estimated. *Nature Communications*, *12*(1), 2501. https://doi.org/10.1038/s41467-021-22702-2

Worden, S., Bloom, A. A., Worden, J., Levine, P., Shi, M., & Fu, R. (2024). Congo basin water balance and terrestrial fluxes inferred from satellite observations of the isotopic composition of water vapor. *Water Resources Research*, *60*(7), e2023WR035092. https://doi.org/10.1029/2023WR035092

Worden, S., Fu, R., Chakraborty, S., Liu, J., & Worden, J. (2021). Where does moisture come from over the Congo basin? *Journal of Geophysical Research: Biogeosciences*, *126*(8), e2020JG006024. https://doi.org/10.1029/2020JG006024

Wunderling, N., Staal, A., Sakschewski, B., Hirota, M., Tuinenburg, O. A., Donges, J. F., et al. (2022). Recurrent droughts increase risk of cascading tipping events by outpacing adaptive capacities in the Amazon rainforest. *Proceedings of the National Academy of Sciences*, *119*(32), e2120777119. https://doi.org/10.1073/pnas.2120777119

Xiao, M., & Cui, Y. (2021). Source of evaporation for the seasonal precipitation in the Pearl River Delta, China. *Water Resources Research*, *57*(8), e2020WR028564. https://doi.org/10.1029/2020WR028564

19447973, 2026, 9, Downloaded from https://agupubs.onlinelibrary.wiley.com/doi/10.1029/2025WR043039 by Technical University Delft, Wiley Online Library on [10/09/2026]. See the Terms and Conditions (https://onlinelibrary.wiley.com/terms-and-conditions) on Wiley Online Library for rules of use; OA articles are governed by the applicable Creative Commons License

Yang, J., Tian, H., Pan, S., Chen, G., Zhang, B., & Dangal, S. (2018). Amazon drought and forest response: Largely reduced forest photosynthesis but slightly increased canopy greenness during the extreme drought of 2015/2016. *Global Change Biology*, *24*(5), 1919–1934. https://doi.org/10.1111/gcb.14056

Yang, Z., & Dominguez, F. (2019). Investigating land surface effects on the moisture transport over South America with a moisture tagging model. *Journal of Climate*, *32*(19), 6627–6644. https://doi.org/10.1175/JCLI-D-18-0700.1

Zangvil, A., Portis, D. H., & Lamb, P. J. (2004). Investigation of the large-scale atmospheric moisture field over the midwestern United States in relation to summer precipitation. part ii: Recycling of local evapotranspiration and association with soil moisture and crop yields. *Journal of Climate*, *17*(17), 3283–3301. https://doi.org/10.1175/1520-0442(2004)017<3283:iotlam>2.0.co;2

Zemp, D. C., Schleussner, C.-F., Barbosa, H. M., Hirota, M., Montade, V., Sampaio, G., et al. (2017). Self-amplified Amazon forest loss due to vegetation-atmosphere feedbacks. *Nature Communications*, *8*(1), 14681. https://doi.org/10.1038/ncomms14681

Zemp, D. C., Schleussner, C.-F., Barbosa, H. M. J., van der Ent, R. J., Donges, J. F., Heinke, J., et al. (2014). On the importance of cascading moisture recycling in South America. *Atmospheric Chemistry and Physics*, *14*(23), 13337–13359. https://doi.org/10.5194/acp-14-13337-2014

19447973, 2026, 9, Downloaded from https://agupubs.onlinelibrary.wiley.com/doi/10.1029/2025WR043039 by Technical University Delft, Wiley Online Library on [10/09/2026]. See the Terms and Conditions (https://onlinelibrary.wiley.com/terms-and-conditions) on Wiley Online Library for rules of use; OA articles are governed by the applicable Creative Commons License